RICE UNIVERSITY

Modeling the influence of large woody debris on delta morphology and longshore sediment transport using the Brazos delta

by

Sarah Huff

A THESIS SUBMITTED
IN PARTIAL FULFILLMENT OF THE
REQUIREMENTS FOR THE DEGREE

Master of Science

APPROVED, THESIS COMMITTEE

Dr. Jeffrey Nittrouer
Assistant Professor, Earth Science, Rice University

Dr. John Anderson
Professor, Earth Science, Rice University

Dr. Caroline Masiello
Professor, Earth Science, Rice University

Dr. Jorge Lorenzo-Trueba
Assistant Professor, Earth and Environmental Studies, Montclair State University

HOUSTON, TEXAS
April 2015

RICE UNIVERSITY

Modeling the influence of large woody debris on delta morphology and longshore sediment transport using the Brazos delta

by

Sarah Huff

A THESIS SUBMITTED
IN PARTIAL FULFILLMENT OF THE
REQUIREMENTS FOR THE DEGREE

Master of Science

APPROVED, THESIS COMMITTEE

Dr. Jeffrey Nittrouer
Assistant Professor, Earth Science, Rice University

Dr. John Anderson
Professor, Earth Science, Rice University

Dr. Caroline Masiello
Professor, Earth Science, Rice University

Dr. Jorge Lorenzo-Trueba
Assistant Professor, Earth and Environmental Studies, Montclair State University

HOUSTON, TEXAS
June 2015

Abstract

Modeling the influence of large woody debris on delta morphology and longshore sediment transport using the Brazos delta

by Sarah Huff

The role of large woody debris (LWD) in coastal sediment dynamics is understudied, but yet is an important consideration in the face of modern climate change and coastal erosion. In addition to amplified aeolian sediment capture due to increased roughness of the shoreface, LWD has implications for reducing sediment transport capacity along the shoreface, thereby stabilizing sediment and minimizing long-term erosion. Here, we examine the impact of LWD concentration within the littoral zone, and relate this to differential longshore sediment transport rates. We hypothesize that LWD concentration and longshore sediment transport are linked. Using a numerical model constrained by data collected from field studies, our results show that increased LWD at the shoreface is inversely related to longshore sediment transport rates. Increased roughness due to LWD results in the loss of stress available to mobilize sediment. Our model allows for first-order predictions of longshore sediment transport based on LWD concentrations at the shoreline.

Field surveys of the modern Brazos river delta in the Gulf of Mexico reveal an abundance of LWD along the coastline and within the delta matrix. There is a multitude of time varying aerial photographs and bathymetric maps that are used to document the relative stability of the modern Brazos River delta despite variable sediment discharge and a similar wave climate that resulted in the rapid erosion of the pre-engineered-diversion, “old” Brazos delta. Despite the similar sediment volume and wave climate characteristics, the modern and old Brazos deltas demonstrate very different morphological histories during times of relaxed sediment discharge. Here we use three modeling approaches to propose that the large quantities of LWD present on the modern delta could dampen longshore sediment transport at the delta shoreface, and thereby stabilize the delta morphology despite an energetic wave climate.

Acknowledgements

This work was completed with the support of my family, friends, and mentors along with funding from Rice University's Shell Center for Sustainability. Each interaction during these past two years shaped my experience at Rice and, in turn, who I am as a scientist and a person. Foremost, I thank my advisor Jeffrey Nittrouer for his wealth of knowledge and currency of ideas throughout this process. His motivation helped drive this project and assisted me in becoming a more well-rounded researcher. I am grateful for Jorge Lorenzo-Trueba, whose unwavering patience, support, and positivity were integral parts of my success. Both John Anderson and Carrie Masiello provided me with a sounding board for ideas ranging from sediment composition to wood decomposition and helped me identify the importance of my project across specializations. I appreciate the discussions with and guidance from all of my committee members and other members of Rice faculty and staff; their knowledge and expertise were crucial components of my success.

I am extremely privileged to have had the love and support of my friends and family throughout this process. Thank you to my labmates, the Sediment Sisters: Tian Dong, Stacy Dwyer, Kaitlin Moran, Brandee Carlson, Andrew Moodie, Brian Demet, Ruthie Halberstadt, Lindsay Prothro, Becky Minzoni, Pankaj Khanna, Maya Stokes, and Christina Hughes. I thank all of the Sediment Sisters for sticking with me during the long days in the field and in the office. I am also infinitely grateful for my friends outside of my lab group, especially Laura Carter, Meghan Byrnes, and Ryan Nupen, without whom I would be lost. The laughter and camaraderie within my friend groups was extremely meaningful and kept me afloat like large woody debris in a storm. I would also like to thank my grandparents; my aunts and uncles; my cousins; and especially my parents, Michael and Michelle; and my sisters, Stephanie and Emily; for their unwavering love, confidence, and support of my endeavors fueled by curiosity.

As Zora Neale Hurston wisely noted, "Research is formalized curiosity. It is poking and prying with a purpose." I have appreciated this opportunity to poke and pry and delve into research that has the potential to positively impact our changing world.

Table of Contents

List of Equations

List of Figures

List of Variables

a	Sediment Packing here taken to be 0.6
B	Volumetric large woody debris (LWD) concentration
C	Combined parameters of the CERC formula ($m^{0.5}/s$)
C_d	Drag coefficient associated with LWD concentration
C_n	Wave group velocity (m/s)
D	Basin depth (m)
E	Wave energy (J/m^2)
γ	Diffusivity (m^2/month)
γ_b	Breaker index, here assumed to be 0.78
H	River mouth location (m)
I_t	Immersed sediment transport (kg/month)
K	Non-dimensional proportionality constant empirically found to be 0.39
q	Sediment flux (m^2/month)
q_a	Longshore sediment flux (m^2/month)
q_{in}	Sediment flux input from historical river discharge data (m^2/month)
Q	Discharge (m^3/month)
s	Shoreline distance from datum (m)
t	Time (months)
τ_b	Stress initially available in the system or boundary shear stress (Pa)
τ_{fd}	Stress removed by drag or form drag stress (Pa)
τ_{sf}	Stress available to move sediment or skin friction stress (Pa)
θ	Angle between wave break and the shoreface
x	Horizontal distance in the modeling framework
W	River width (m)

1. Introduction

Large woody debris (LWD) plays an important role in upland fluvial and lowland estuarine ecosystems by contributing to habitat stability over a wide range of water discharge regimes and environmental energies (Abbe and Montgomery, 1996, Angradi et. al., 2004). The influence of LWD in upland river channels has been well studied, and the outcome of this research has provided a better understanding for how the sequestration of wood affects local food webs, as well as influences water and sediment discharge (Heede, 1985; Smith et. al., 1993; Assani and Petit, 1995; Shields and Gippel, 1995, Gippel et al., 1996; Abbe, 2000; Manga and Kirchner, 2000; Montgomery and Piegay, 2003). To this aim, numerous studies and experiments have been designed from which empirical relationships have been developed to describe the relationship between the concentration of LWD and reduction of sediment transport (Shields and Gippel, 1995, Abbe and Montgomery, 1996, Booth et al, 1997, Gurnell et. al., 2002). For example, in channelized flow, LWD acts to attenuate flow energy through absorption and reflection of fluid energy, ultimately resulting in a reduction of flow velocity and sediment transport capacity (Cherry and Beschta, 1989, Shields and Gippel, 1995; Hygeland and Manga, 2003).

Although these upland systems have been well studied, the effect of LWD on coastal morphology is as not well understood. Despite a lack of quantitative constraint regarding the effects of LWD on coastal shorefaces, LWD has been artificially placed on shorefaces as a low-cost technique to mitigate shoreface erosion by decreasing longshore transport. Often, "conventional wisdom" is cited as the reasoning behind such actions (Zelo et al., 2000). Recent research of coastal regions using LiDAR data has shown that LWD increases roughness over the dry shoreface and works to trap sediment transported by aeolian processes (Eamer and Walker,

2010; Heathfield and Walker, 2011). However, the LWD's influence on longshore transport – the wetted portion of the shoreface – has yet to be explored (Eamer and Walker, 2010). This research aims to elucidate the effects of LWD on longshore sediment transport, and describe its effect on delta morphology.

Here, we take advantage of a natural experiment of the Brazos River delta engineered diversion (Texas, U.S.A.), whereby one delta was destroyed and a new delta created in the time frame of decades, to provide a mechanistic understanding of this "conventional wisdom" used to justify shoreface engineering designs. The modern Brazos River delta is unique because it provides the opportunity to evaluate delta evolution via shoreface sediment transport while considering both an abundance and lack of LWD. We first seek to identify a relationship between LWD and longshore sediment transport, so to capture the evolution of the Brazos River delta system through numerical modeling efforts. We then relate these findings to a mechanistic sediment transport model. Field surveys and time-lapse photographs are used to provide data that inform and validate our numerical modeling approach.

2. Regional Setting

2.1 Study area setting

The modern Brazos delta is located on the upper Texas coast near the town of Surfside, which is located about 100 kilometers south-southwest of Houston (Figure 1). The delta is comprised of ~ 50% prodelta-muds and ~ 50% fine sand (Rodriguez et. al., 2000). Previous field studies have observed an inner matrix of LWD within the modern delta framework that approximately mirrors the active shoreface composition of LWD, which is known to vary in size and concentration (Anderson, 2014, personal communication).

Classically defined as a wave-dominated delta system, the Brazos system is characterized by a wave climate where swell approaches from a southeastern direction with a mean significant height of 0.85 m, and mean peak period of 5.3 s, as determined by 25 years of hindcast data (USACE, WIS 73064). The system experiences a diurnal microtidal environment with an amplitude of 0.5 m (NOAA, Station ID 8772447).

2.2 Study area history

The Brazos River basin encompasses approximately 118,000 km^2 and spans from eastern New Mexico across Texas, before entering the Gulf of Mexico (Figure 1, Fraticelli, 2006). This geographic region covers a wide range of climate and precipitation gradients (Rodriguez et. al., 2000). The climate variability produces relatively prolonged periods of low flow (multiple years) that are punctuated by flood events, whereby the largest flood events typically occur over decadal time scales and are associated with El Niño events (Rodriguez et. al., 2000). The majority of time, however, the arid climate persistent across much of the Brazos basin produces minimal river water discharge. For example, USGS data spanning from 1903 until present show that the Brazos River water discharge is approximately 2390 m^3s^{-1} at its peak, but a more typical discharge, accounting for over 70 % of the flow period, is below 250 m^3s^{-1} (Figure 2, Strom and Rouhnia, 2013). The nature of the Brazos River is therefore defined by high-intensity discharges that interrupt long periods of low flow.

Brazos River flood events transport a large volume of sediment to the river-ocean interface. During low flow events, however, sediment flux to the delta front is minimal to nonexistent (Strom and Rouhnia, 2013). Despite this condition of punctuated sediment transport, the Brazos River maintains the highest average annual sediment load delivered to the Gulf of Mexico for all Texas rivers (Fraticelli, 2006). Water discharge is related to sediment discharge

through a power law function developed using sediment concentration and water discharge data collected at Richmond, TX, located approximately 80 km upstream of the Brazos River outlet (Figure 3). This relationship is used to estimate sediment flux based on daily measured water discharge data (Figure 4).

Due to its proximity to agricultural regions of Texas, the Brazos River is a valuable resource for transporting commercial products. However, the river was not always easily navigated, especially in the lower region, due to reoccurring log jams and river shoaling. Therefore, dredging and log collecting along the banks was required to maintain the river for navigation (Alperin, 1977). To aid the navigation effort, in 1929, the Brazos River was artificially diverted so to debouch 6.5 kilometers to the south. In approximately 11 years (1940), the old delta was completely destroyed due to erosion by wave energy (Figure 5, Seelig and Sorensen, 1973; Rodriguez et al., 2000; Watson, 2003). Today, the same wave energy that eroded the old delta remains, however the modern delta has established and remains stable despite extended low-flow periods when little sediment is discharged to the Gulf of Mexico (Gibeaut et al., 2000). Interestingly, the length of time over which these low flow conditions persist often scale to the time period for which all geomorphic evidence of the old delta was removed (i.e., multiple years).

The modern Brazos delta has developed more or less as a result of major river floods occurring decadally in association with El Nino events (Rodriguez et al., 2000). The sediment delivered to the delta during flood events, in particular, the relatively coarser sand fraction, “welds” onto the coastline as a result of longshore transport processes, thereby growing the modern Brazos delta over time through the development of beach ridges (Rodriguez et al., 2000). These ridges persist as topographic features of the delta, whereby each ridge represents a

previous coastal interface, and the swales (i.e., topographic lows between the ridges) are regions of active overwash (mud) sedimentation (Rodriguez et al., 2000). During periods of low sediment discharge, the morphology of the delta is modified due to some coastal erosion along the active shoreface. Interestingly, despite the rapid erosion of the old delta (destroyed in 11 years after the engineered diversion), one could expect there to be significantly more modification to the modern delta, particularly during prolonged droughts that last between five to ten years. Despite essentially nil sand discharge to the mouth of the Brazos River during multiple droughts, the modern delta has maintained a relatively stable morphology.

The modern Brazos River delta system possesses a significant concentration of LWD within both the delta sediment matrix and at the coastal shoreface. Much of this LWD, like in many fluvial systems, is sourced from trees along the eroding banklines of the upstream river system (Figure 6, Phillips, 2006). The Brazos River is no outlier in this regard: the LWD has always been prevalent, and the sinuous nature of the old channel sequestered so much LWD in the bends of the lower reach that constant removal of large log jams was cited as a primary reason for diverting and straitening the river to its modern location (Alperin, 1977). This engineering design (i.e., straight channel) enables for efficient transport of LWD and sediment to the outlet, thereby clearing the main channel for navigation.

2.3 Study site location rationale

The Brazos River coastal morphology has been well documented over the past century via extensive aerial photography. Additionally, numerous field studies have been conducted, examining the morphological and stratigraphic development of the Brazos delta, particularly in regard to the water and sediment events that feed the delta system (Rodriguez et. al., 2000; Fraticelli, 2006; Strom and Rouhnia, 2013; Keel, 2014). The Brazos River delta system is an

ideal candidate for examining fluvial-deltaic processes because it is possible to compare the temporal evolution of both the old and modern deltas, and therefore evaluate the role of sediment flux and LWD in terms of delta stability.

3. Methods

3.1 Numerical Delta Model

3.1.1 Governing Equations and Boundary Conditions

A numerical delta model following the CERC formulation is used here to evaluate the spatiotemporal evolution of the old and modern Brazos deltas. The model is outlined by the USACE in their 1984 Shore Protection Manual:

Equation 1

$$Q = KH^{5/2} \sin 2\theta \frac{\rho_{f\sqrt{g}}}{16\sqrt{\gamma_b}(\rho_s - \rho_f)(0.6)}$$

where Q is the volumetric sediment transport rate in cubic meters per second, K is an empirically defined proportionality constant, H is significant wave height in meters, theta (θ) is the breaking angle between the wave crest and the shoreface, γ_b is the breaker index which is set here set to be 0.78, ρ_f is the fluid density (1020 kg/m^3), ρ_s is the sediment density (2650 kg/m^3), g is gravitational acceleration (9.81 m/s^2), and a is sediment packing ratio typically taken as 0.6, implying that granular packing allows for 40% void space. We can combine some of these parameters into a single value, C, because we assume they remain constant over the duration of the model run, where C is defined as:

Equation 2

$$C = K \frac{\rho_{f\sqrt{g}}}{16\sqrt{\gamma_b}(\rho_s - \rho_f)(a)}.$$

After combining these parameters, the remaining variables are wave energy and wave breaker angle. To characterize the net effect of these controls we use diffusivity (γ), in meters squared per month:

Equation 3

$$\gamma = \frac{CH^{5/2}}{D}$$

where diffusivity is a function of *C*, a term that combines wave height (*H*) and the basin depth. Using this diffusivity parameter, longshore sediment transport rates, *q*, are calculated:

Equation 4

$$q = -\gamma \frac{\delta s}{\delta x}$$

where q is sediment transport ($m^2\ s^{-1}$), s is the shoreline distance from the datum (m), and x is the horizontal distance from the datum (m). Here we assume that the angle of the shoreface (i.e., $\frac{\delta s}{\delta x}$) and the breaker angle (θ) are equivalent.

In our model, shoreline movement over time is a function of sediment transport along the shoreline:

Equation 5

$$\frac{\partial s}{\partial t} = -\frac{\partial q}{\partial x}.$$

The governing equation for all sites along the horizontal axis is a modified version of the Exner equation (Ashton and Giosan, 2011):

Equation 6

$$\frac{\partial s}{\partial t} = \gamma \frac{\partial^2 s}{\partial x^2}.$$

The change in shoreline over time is a function of wave climate and the change in slope with respect to the horizontal distance from the datum. Our boundary condition is set by the longshore sediment flux starting from the river mouth (x=0), which is initially a function of the river width (W), basin depth (D), and sediment input from the river (q_{in}), so that:

Equation 7

$$\gamma \frac{\delta s}{\delta x} \Big|_{x=0} = -\frac{W}{2}\frac{q_{in}}{D}.$$

Therefore, the river mouth location and the shoreline (s) start at x=0 and evolve over time as:

Equation 8

$$q_{in} - q_a = D\frac{ds_{x=0}}{dt}.$$

Ultimately, the change in river mouth location is a balance between the sediment input at the river mouth (q_w) and the sediment transported alongshore through longshore sediment transport (q_a).

The model is evaluated for the modern system by using sand flux calculated for the Brazos River based on the discharge and sediment flux rating curves described above (Figure 2, Figure 3, Figure 4), and considers one-half of the symmetric delta model to compare to the evolution of the modern system over time, because here we evaluate the portion of Brazos delta removed from anthropogenic influence (i.e., the western half). The initial condition for the modern delta considers a shoreline position that starts at x=0 and evolves over time, whereby the

modeled position of the river mouth and shoreface is validated based on aerial photographs of the modern Brazos delta. We also model erosion of the old Brazos delta, where the model starting point is determined by aerial photographs at the time of the engineered diversion in 1929. These pictures show that the old delta protruded 2 km into the Gulf of Mexico, and had an alongshore length of approximately 8 km (Figure 7).

3.1.2 Numerical Method

The delta shoreline evolution is determined by iteratively solving the sediment transport equations at each location on the established grid, following the model style of Komar (1973). Our model is implemented using the Euler numerical method. An imposed boundary condition is that at time t=0, the shoreline at the river mouth is 0 m from the shoreline datum, and sediment flux at the initial river mouth is defined by:

Equation 9

$$q_1 = \frac{W}{2} * \frac{q_{in} - \dot{s_1} * D}{D}$$

where q_1 is the sediment flux at the first node of the delta grid, W is the river width —equal to a constant 250 m based on measurement, q_{in} is the fluvial sediment input which varies through time based on the historical monthly data from the Richmond USGS station, (Figure 4 and Figure 8). s_1 is the river mouth location or the shoreline location at the first node. The total basin depth (D) is 8 m, however the sandy sediment in this coastal region are only noted in the upper 4 m, and so we use this value as our depth of sand closure (Wallace et. al., 2010; Anderson, Personal Communication 2014).

We assume that the long-term wave climate has remained consistent because there is little evidence to imply otherwise, as bolstered by long-term wave energy data, measured by

USACE buoy data, which show no trend since data collection commenced in 1980 (Figure 5). We also assume there have been no significant anthropogenic influences at the shoreface; this condition is met because the modern Brazos delta is undeveloped and removed from anthropogenic influence. Additionally, we also assume that a significant portion of the longshore sediment transport occurs at the beach shoreface (i.e., breaker zone), and that the total sediment flux may be calculated based on the shoreface change that is integrated to the depth of sand closure. Sediment measurements from the delta show that the composition is approximately 50% sand and 50% mud. Therefore we assume that the sediment discharge contributing to delta growth is comprised of all of the measured sand discharge, plus an equal volume of mud (Rodriguez et. al., 2000).

Based on aerial photographs of the delta, and using a total sediment storage depth of 8 m (the pre-diversion basin depth), the estimated volume of sediment for the western half of the modern delta is 8.10×10^7 m^3. Based on Brazos River sediment flux data, and assuming a sediment capture by the modern delta that is 50% sand and 50% mud, the cumulative volume of stored sediment for the western side of the delta is calculated as approximately 7.13×10^7 m^3. The similarity between the estimated sediment volume based on aerial photographs and the volume based on river sediment discharge affirms the validity of our assumption that the western half of the system functions as one-half of a symmetric delta, and consists of proportional amount of sediment delivered by the Brazos River.

Our numerical shoreline evolution equation (Equation 6) is implemented as:

Equation 10

$$\frac{\delta s}{\delta t} = -D^{-1} * \frac{\delta Q}{\delta x}.$$

Within this model, shoreline position over time is modified as a function of depth and sediment transport over a defined distance x so that *s* is the shoreline position, in meters, from the datum, *t* is time, in months, δx is the change in horizontal position in meters across the datum, equal to 800 m, *D* is designated as the sand depth of closure, set to 4 m, and δQ is the difference in longshore sediment transport rates (m^3 /month). The change in longshore sediment transport rate is determined by:

Equation 11

$$\delta Q = (q_{i-1} * D_{i-1}) - (q_i * D_i)$$

where the change in longshore transport rate (δQ) over a section of delta is attributed to a change in longshore sediment flux (m^2/month)(q), multiplied by the depth of closure (*D*). Substituting for q where:

Equation 12

$$q = -\gamma \frac{s_{i+1} - s_i}{\delta x}.$$

Sediment flux is controlled by the change in shoreline distance from the datum for a change in horizontal distance, which is controlled by the diffusive term, γ, which characterizes the longshore flux of sediment over the delta. Localized sediment flux is dependent on this diffusive term and the change in shoreline over change in space for each delta section is:

Equation 13

$$\delta Q = -\gamma \left(\frac{s_i - s_{i-1}}{\partial x} * D_{i-1}\right) + \gamma \left(\frac{s_{i+1} - s_i}{\partial x} * D_i\right).$$

Therefore, change in sediment transport at each delta node is a function of the diffusive term, the delta's shoreline gradient (i.e., the difference in shoreline distances from the datum) and the depth of closure.

If the sediment transport rate is greater entering into a cell than leaving the cell (i.e., a net-positive rate), as determined using Equation 13, the location of the shoreline (*s*) from the datum will increase. Intrinsically, higher diffusivity rates result in much slower rates of shoreline growth as the higher diffusivity leads to greater sediment transport from of all cells, thereby outpacing the sediment input from the river mouth.

3.2 Field Methods

3.2.1 Calculating concentration of LWD

We determine the approximate concentration of LWD located along shoreface of the Brazos delta through targeted surveys. Eleven discrete sampling sites were determined, and the alongshore length of each survey site is based on statistically sufficient sampling count of individual tree logs that comprise the LWD (i.e., $n>30$). The width of each survey site is contained by the intertidal zone, so the mean low-tide shoreface to the limit of debris, which is identified as the high high-tide wood rack line. At each site, the length and circumference of all logs were measured to constrain an approximate LWD volume, and the total LWD volume is the sum of all measured logs. The survey site volume is the estimated as the product of the area and a storage depth, approximated to be 0.5 m (Eamer and Walker, 2010). LWD concentration is evaluated as the quotient of LWD volume and survey site volume.

3.2.2 Calculating sediment flux based on shoreline change

The Brazos River delta shoreline was discretized into 13 500-m regions for sediment transport analysis (Figure 9A), which is a spatial step that adequately captures sinuosity of the shoreline (Figure 9A). Shoreline migration rates for the modern Brazos delta were calculated for each 500-m along-shore regions across the delta. For each of these regions, LWD concentration was estimated based on a weighted average of the measured LWD concentrations from the field survey sites (Figure 9B). For each 500-m region, Google Earth images from May 2014 and

February 2010 were compared to measure the difference in the seaward-most permanently subaerial region of the coastline (i.e., the region not influenced by tides). The average monthly change in sediment volume over the 51-month time period was determined for each 500-m region, based on the respective shoreline changes, multiplied by the depth of closure for sand (4 m). Ultimately, the relationship between change in shoreline position (*s*) and change in sediment transport (q) can be described as:

Equation 14

$$\frac{(\delta s)(l_r)}{\delta t} = \delta q.$$

The median change in shoreline position (δs) for the length of the region (l_r) (here established as 500 m) over a period of time (δt) is equal to the change in sediment transport (δq) over that same period because depth is held constant. The spatial variability of these sediment transport changes are then related to the measured LWD concentrations.

3.3 Relating LWD concentration and modeled sediment flux

To relate LWD concentration to changes in sediment flux for the Brazos River delta, we utilize existing models that estimate sediment transport. We outline both an energetics-based model, and mechanistic sediment transport models, and use measured changes in sediment transport rates to confirm and validate these model approaches.

3.3.1 Modeling longshore sediment transport equations using an energetics model

To model longshore sediment transport rates for this system we use the fundamental work of Inman and Bagnold (1963). The relationship describes the immersed-weight sediment transport rate (I_t) (kg/month) and the wave climate is given as:

Equation 15

$$I_t = K(EC_n)\sin\theta\cos\theta$$

where K is a dimensionless proportionality coefficient, E is the energy (J/m^2) of the breaking waves, C_n is the group wave velocity (m/month), and θ is the angle between the shoreline and the breaking waves (Inman and Bagnold, 1963). The validity of the equation as well as the value of K, which has been found to range from 0.39 to 0.77, has been established by the field measurements of Komar and Inman (1970; Komar, 1971). We relate the immersed-weight sediment transport rate to a volumetric sediment transport rate (S) (m^3/month) using:

Equation 16

$$S = \frac{I_t}{(\rho_s - \rho_f) g a}$$

(Komar and Inman, 1970).

These equations are translated to the CERC formula (Equation 1) from the USACE's Shore Protection Manual (1984) and allow us to calculate a volumetric sediment transport rate based on significant wave height. We calculate the expected longshore sediment transport rate for each region and compare the rates spatially. This allows us to determine the negative (erosive) and positive (progradational) change in sediment transport divergence patterns between the regions. We can then use these values and change in sediment transport divergence patterns along the shoreface and observe if they compare favorably to the values measured using the time-lapse images.

3.3.2 Calculating stress and sediment transport based on a mechanistic model

Relationships between sediment transport stress and LWD have been established for environments of channelized flow. Here we assume that the wave energy driving sediment transport is focused in a uniform direction, and so these previously established relationships can be extended for use in our study. Although wave energy is the primary driver of longshore sediment transport, LWD attenuates sediment transport by increasing roughness and therefore

form drag, thereby lowering the sediment transport capacity by decreasing stress available for sediment transport. For example, Dietrich and Smith (1984) and Nelson and Smith (1989) show that the stress applied by a moving fluid available to transport sediment (τ_{sf}) is a function of the total boundary stress (τ_b) minus the form drag stress (τ_{fd}):

Equation 17

$$\tau_{sf} = \tau_b - \tau_{fd}.$$

To quantify the form drag of LWD we first utilize the relationship of Gippel et al. (1996) to evaluate the drag coefficient:

Equation 18

$$C_d = 0.6 * \left(0.997 * (1 - B)^{2.06}\right)^{-1}$$

where *B* designates the LWD concentration in the region affected by fluid stress, and C_d is the resulting drag coefficient. C_d relates is then related to form drag (τ_{fd}) through:

Equation 19

$$\tau_{fd} = \frac{1}{2}\rho C_d u_*^2$$

where u_* refers to the fluid shear velocity.

We calculate the sediment flux utilizing three physically based sediment transport equations: Ashida and Michiue (1972), Wilson (1966), and Wiberg and Smith (1989). First we consider Ashida and Michiue's (1972) equation:

Equation 20

$$q^* = 17(\tau_b^* - \tau_{cr}^*)\left(\sqrt{\tau_b^*} - \sqrt{\tau_{cr}^*}\right)$$

where q^* is dimensionless sediment transport rate, τ_b^* is dimensionless boundary shear stress, and τ_{cr}^* is dimensionless shear stress for a grain size of 125 microns, which represents the median diameter (D_{50}) along the Brazos delta shoreface (Hamilton, 1995). Ashida and Michiue (1972)

do not consider form drag, so we substitute τ_{sf}^* for τ_b^* using Equation 17 to approximate the stress available for sediment transport, after accounting for LWD form drag, using Equation 18, and Equation 19.

Sediment transport is also calculated using the Wilson (1966) formulation, after accounting for form drag associated with the LWD where:

Equation 21

$$q^* = 12(\tau_{sf}^* - \tau_{cr}^*)^{1.5}.$$

Wiberg and Smith (1989) also provide a physically based relationship for the sediment transport and, again, we account for LWD form drag, where:

Equation 22

$$q^* = (1.6\ln\tau_{sf}^* + 9.8)(\tau_{sf}^* - \tau_{cr}^*)^{1.5}.$$

To convert from dimensionless (q^*) to dimensional (q) sediment transport, it is necessary to consider median grain size (D_{50}), and sediment and fluid densities (Shields, 1936):

Equation 23

$$q = (q^*)\left(\sqrt{\left(\frac{\rho_s - \rho_w}{\rho_w}\right) g {D_{50}}^3}\right).$$

We seek to calculate sediment transport rates for the delta based on the variable form drag associated with the measured of LWD concentration. Using these values, we calculate the negative divergence (implying erosion) or positive divergence (implying progradation) based on change in sediment transport rates by comparing each region to its neighboring down-drift region. This method of evaluating the change in sediment transport rates based on the above three sediment transport equations can then be compared to the measured change in sediment transport rates using aerial photography as described above (i.e., Equation 14), and considering the appropriate time frame (i.e., *t*=51 months) and those calculated using the CERC formula.

4. Results

4.1 Numerical Delta Modeling Results

Despite the similar morphological characteristics of the old and modern Brazos deltas, a single applied diffusivity rate (γ) corresponding with a single energy flux does not allow the model to replicate the known historic shoreline changes for both systems. To build the delta to its modern position and coincide with an appropriate range of the historical shoreline data, the delta requires a diffusivity value of 22,500 m^2/month (Figure 10 and Figure 11). However, this diffusivity value does not allow the old delta to erode within its appropriate time frame, i.e., 11 years. For example, if a diffusivity value of 22,500 m^2/month is applied to the old delta, the model shows that it would not fully erode before 2013 (Figure 12). In order to produce the complete erosion of the old delta over the known eleven year time frame, a diffusivity of 225,000 m^2/month is required. However this diffusivity value does not allow for the modern delta to sufficiently prograde (Figure 13, Figure 14, and Figure 15). Therefore, while the erosion of the old Brazos delta system and the progradation of the modern Brazos system are captured with this model, the diffusivity values required to match the observed times of evolution differ by an order of magnitude (Figure 16). Diffusivity values notwithstanding, this simple numerical delta model (Figure 8) not only captures the progradational evolution of the modern Brazos River delta into the Gulf of Mexico, it also replicates the width of the modern delta (approximately 8 km). Provided that the significant wave energy and direction has not changed within the last eight decades, our results imply that the energy driving longshore sediment transport must be attenuated differently between the old and modern delta systems.

4.2 Field results

4.2.1 Concentrations of LWD along the Brazos delta coastline

Regions with higher LWD concentration are located at the river mouth and on the west flank of the delta (Figure 9B, Figure 17, and Figure 18). Interestingly, our field surveys found that portions of the delta were observed to be significantly eroded, so much so that muddy back-bay sediment and associated flora and fauna (e.g., reeds and oysters) were observed adjacent to and within the present breaker zone (Figure 19). Observations of these eroding regions warranted comparing measured changes in local beach sand volume to the local concentration of LWD (Figure 20).

4.2.2 Calculated change in sediment flux from field data and aerial photographs

The Brazos River delta shoreline was broken into 13, 500-m shoreline regions (Figure 9). Based on the magnitude of shoreline migration between February 2010 (Figure 17) and May 2014 (Figure 18), a rate of shoreline migration is calculated for each 500-m region (Equation 14). These values are converted to a sediment transport rate, and then compared to the LWD concentrations estimated for each of the respective regions.

Table 1. LWD concentration and associated shoreline migration and measured change in sand volume sediment from 2010 to 2014

Region (Westernmost to Easternmost)	LWD Concentration	E Location of Midpoint (UTM)	N Location of Midpoint (UTM)	Measured Shoreline Migration (m) (2010-2014) (Negative Values Indicate Erosion)	Measured Rate of Change in Transport (m^2/month) (Negative Values Indicate Erosion)
1	0.07	262387	3194162	25	245
2	0.07	262867	3194308	16	157
3	0.17	263346	3194456	13	127

4	0.32	263823	3194617	-3	-29
5	0.47	264297	3194773	5	49
6	0.63	264767	3194946	-10	-98
7	0.02	265236	3195124	-13	-127
8	0.01	265695	3195325	-21	-206
9	0.05	266158	3195523	-72	-706
10	0.06	266614	3195722	-84	-824
11	0.07	267079	3195909	-140	-1373
12	0.00	267535	3196106	-215	-2108
13	0.78	267789	3196509	-28	-275

4.3 Sediment transport rates related to LWD

4.3.1 Modeled longshore sediment transport based on volumetric sediment transport equations

For calculating longshore sediment transport, and changes in longshore sediment transport based on the CERC formula, we require a set of inputs specific to the Brazos delta system (Table 2).

Table 2. Input variables for calculating longshore sediment transport using the CERC formula

Input parameter	Value	Units	Description
K	0.39		Non-dimensional proportionality constant
H	0.25	M	Approximated significant wave height at the shoreface
EC_n	1.13×10^{8}	Erg/cms	Wave Energy Flux Calculated from buoy data
A	0.6		Correction for Porosity
G	-9.81	m/s^2	Gravitational acceleration
ρ_s	2650	kg/m^3	Density of sediment
ρ_w	1020	kg/m^3	Density of water
θ	Varies based on location	Degrees	Angle between wave crest (122.85 degrees) and the shoreface
B	Varies based on location		Concentration of LWD at the shoreface

Based on the longshore sediment transport equation developed the USACE (1984), the calculated average longshore sediment transport rate for the Brazos delta system is -1745 m^2/month (negative value indicates erosion) for each 500 m region; this assumes an average 21° angle between the wave-break and the shoreline, and holds wave energy flux at 1.13×10^8 erg

cm^{-1} s^{-1}, the calculated energy flux based on data from the USACE buoy (WIS 73064, UTM 15R 290262 E 3193266 N) 24 km away. However, a single sediment transport rate does not capture the nature of the shoreface, which is naturally sinuous, and a constant rate implies a pattern of constant sediment divergence along the delta shoreface. If we calculate sediment transport rates using the range of angles between wave-break and the shoreline within each 500-m region, we can appropriately compare the change in these calculated rates to our observed change in sediment transport rates (Table 3).

Table 3. Sediment transport rates calculated using the CERC formula

Region	LWD Concentration (*B*)	Breaker Angle Between Wave Crests and the Shoreface	CERC Formula Calculated Sediment Flux (assuming a depth of 4 m) (m^2/s)	Change in Sediment Flux (m^2/s) between neighboring regions, based on the CERC calculated fluxes for each region	Measured Change in Sediment Flux Based on Aerial Photographs (m^2/s)
1	0.07	9	6.71E-04	6.71E-04	9.46E-05
2	0.07	9	6.72E-04	7.35E-07	6.05E-05
3	0.17	9	6.72E-04	7.27E-07	4.92E-05
4	0.32	9	6.73E-04	4.86E-06	-1.13E-05
5	0.47	10	6.78E-04	6.61E-07	1.89E-05
6	0.63	10	6.79E-04	-2.43E-05	-3.78E-05
7	0.02	7	6.54E-04	-1.98E-05	-4.92E-05
8	0.01	5	6.35E-04	4.96E-05	-7.94E-05
9	0.05	11	6.84E-04	-2.99E-05	-2.72E-04
10	0.06	7	6.54E-04	2.99E-05	-3.18E-04
11	0.07	11	6.84E-04	-7.54E-04	-5.30E-04
12	0.00	-30	-7.00E-05	-2.13E-04	-8.13E-04
13	0.78	-39	-2.83E-04	2.83E-04	-1.06E-04

Comparing the results for regional change in sediment flux, based on CERC model results for each region, to the measured change in sediment flux, we observe that the CERC formula

overestimates sediment transport along the delta and does not fully capture the dynamism of the shoreline over time, although it does capture general patterns of erosion (Figure 21). This could be due to the extreme sensitivity of the formula to the angle between the wave crest and the shoreface, whereby the wave angle is variable and may produce divergent sediment fluxes (Figure 22). To gain a better understanding of the evolution of the Brazos River delta shoreline, we should examine the influence of LWD on the mechanics of sediment transport, and evaluate if the shoreface evolution can be reproduced after accounting for the form drag induced by LWD.

4.3.2 Calculated difference in transport based on LWD concentrations

Boundary stress (τ_b) is approximated for the Brazos delta shoreface by inserting the CERC model sediment transport values for q in an inverted Ashida and Michiue (1972) sediment transport equation (Equation 20), and solving for boundary stress. This method produces an average value of 13 Pa, which is a reasonable expected value at the shoreface, based on previous experiments of breaking waves (Seelam and Baldock, 2009).

Using the Gippel et al. (1996) estimate for drag coefficient (Equation 18) and calculating form drag (Equation 19), in the absence of LWD (i.e., B=0), the estimated value is 3.9 Pa. This value likely accounts for other elements of form drag within the system (e.g., grain to grain interactions, bedforms, etc.). Here we intend to calculate average sediment flux for each of the 500-m regions that comprise the delta shoreface (Figure 9), using the boundary stress defined above (i.e., 13 Pa), and by accounting for the form drag based on each region's LWD concentration (Table 4).

Table 4. Calculated form drag based on LWD concentration

Region	LWD Concentration	τ_{sf} (Pa)	Percent Form Drag Increase due to measured LWD concentration
1	0.07	4.5	84%
2	0.07	4.5	84%
3	0.17	5.8	107%
4	0.32	8.7	161%
5	0.47	14.7	271%
6	0.63	29.6	546%
7	0.02	4.1	76%
8	0.01	4.0	74%
9	0.05	4.3	80%
10	0.06	4.4	81%
11	0.07	4.6	85%
12	0.00	3.9	72%
13	0.78	88.5	1634%

As the concentration of LWD increases, we observe a trend of increasing τ_{fd} (Figure 23), and because the increase in form drag translates to decreasing sediment transport capacity, sediment flux for any given region should also decrease with increasing LWD concentration. In regions with LWD concentration above 0.4, form drag stress (τ_{fd}) in fact exceeds boundary stress (τ_b), and so there is expected to be a shutdown of sediment transport.

If we assume a constant boundary stress (τ_b), and a calculated form drag stress (τ_{fd}) from Gippel et al. (1996) that incorporates LWD concentration, then we may compute a skin friction stress (τ_{sf}) (Equation 17) for use in the sediment transport models of Ashida and Michiue (1972), Wilson (1966), and Wiberg and Smith (1989), so to calculate the sediment transport for each region on the delta. From these calculated values, we determine the spatial change in sediment transport rates (δq) across the shoreface, where δq is equal to q of one region minus the q of the neighboring downdrift region, so to calculate patterns erosion and deposition based on the local divergences in sediment flux (Equation 6 and Equation 14).

Table 5. Calculated change in sediment transport based on Ashida and Michiue (1972) and Gippel et al. (1996)

Region	LWD Concentration (B)	Calculated Sediment Transport Rate with no LWD considered (m^2s^{-1})	Calculated Sediment Transport Rate using τ_b =13 Pa and τ_{fd} based on LWD concentration (B) (m^2s^{-1})	Calculated Change in Sediment Transport Rate using τ_b =13 Pa and τ_{fd} based on LWD concentration (B) (m^2s^{-1})	Measured Change in Sediment Transport Rate (m^2s^{-1})
1	0.07	7.84E-04	6.99E-04	6.99E-04	9.46E-05
2	0.07	7.84E-04	6.99E-04	-1.59E-04	6.05E-05
3	0.17	7.84E-04	5.40E-04	-3.11E-04	4.92E-05
4	0.32	7.84E-04	2.29E-04	-2.29E-04	-1.13E-05
5	0.47	7.84E-04	0	0	1.89E-05
6	0.63	7.84E-04	0	7.57E-04	-3.78E-05
7	0.02	7.84E-04	7.57E-04	1.08E-05	-4.92E-05
8	0.01	7.84E-04	7.67E-04	-3.90E-05	-7.94E-05
9	0.05	7.84E-04	7.28E-04	-1.12E-05	-2.72E-04
10	0.06	7.84E-04	7.17E-04	-2.32E-05	-3.18E-04
11	0.07	7.84E-04	6.94E-04	8.94E-05	-5.30E-04
12	0.00	7.84E-04	7.83E-04	-7.83E-04	-8.13E-04
13	0.78	7.84E-04	0	0	-1.06E-04

The changes in sediment transport rates (δq) along the shoreline can also be calculated using the sediment transport rates calculated for each site based on Wilson's sediment transport equation (1966) (Equation 21).

Table 6. Calculated change in sediment transport based on Wilson (1966) and Gippel et al. (1996)

Region	LWD Concentration (B)	Calculated Sediment Transport Rate with no LWD considered (m^2s^{-1})	Calculated Sediment Transport Rate using τ_b =13 Pa and τ_{fd} based on LWD concentration (B) (m^2s^{-1})	Calculated Change in Sediment Transport Rate using τ_b=13 Pa and τ_{fd} based on LWD concentration (B) (m^2s^{-1})	Measured Change in Sediment Transport Rate (m^2s^{-1})
1	0.07	6.27E-04	5.62E-04	5.62E-04	9.46E-05
2	0.07	6.27E-04	5.62E-04	-1.23E-04	6.05E-05
3	0.17	6.27E-04	4.39E-04	-2.44E-04	4.92E-05
4	0.32	6.27E-04	1.95E-04	-1.95E-04	-1.13E-05
5	0.47	6.27E-04	0	0	1.89E-05
6	0.63	6.27E-04	0	6.06E-04	-3.78E-05
7	0.02	6.27E-04	6.06E-04	8.25E-06	-4.92E-05
8	0.01	6.27E-04	6.14E-04	-2.99E-05	-7.94E-05
9	0.05	6.27E-04	5.84E-04	-8.62E-06	-2.72E-04
10	0.06	6.27E-04	5.75E-04	-1.78E-05	-3.18E-04
11	0.07	6.27E-04	5.58E-04	6.85E-05	-5.30E-04
12	0.00	6.27E-04	6.26E-04	-6.26E-04	-8.13E-04
13	0.78	6.27E-04	0	0	-1.06E-04

Using the relationship developed based on the physical dependence of sediment transport and skin friction stress, Wiberg and Smith's (1989) sediment transport equation can also be used to calculate sediment transport (q) for each region, and these values also used to estimate the change in sediment transport rate (δq) along the shoreface (Equation 22).

Table 7. Calculated change in sediment transport based on Wiberg and Smith (1989) and Gippel et al. (1996)

Region	LWD Concentration (B)	Calculated Sediment Transport Rate with no LWD considered (m^2s^{-1})	Calculated Sediment Transport Rate using τ_b =13 Pa and τ_{fd} based on LWD concentration (B) (m^2s^{-1})	Calculated Change in Sediment Transport Rate using τ_b =13 Pa and τ_{fd} based on LWD concentration (B) (m^2s^{-1})	Measured Change in Sediment Transport Rate (m^2s^{-1})
1	0.07	6.38E-04	5.67E-04	5.67E-04	9.46E-05
2	0.07	6.38E-04	5.67E-04	-1.33E-04	6.05E-05
3	0.17	6.38E-04	4.34E-04	-2.55E-04	4.92E-05
4	0.32	6.38E-04	1.79E-04	-1.79E-04	-1.13E-05
5	0.47	6.38E-04	0	0	1.89E-05
6	0.63	6.38E-04	0	6.15E-04	-3.78E-05
7	0.02	6.38E-04	6.15E-04	9.10E-06	-4.92E-05
8	0.01	6.38E-04	6.24E-04	-3.29E-05	-7.94E-05
9	0.05	6.38E-04	5.91E-04	-9.48E-06	-2.72E-04
10	0.06	6.38E-04	5.82E-04	-1.96E-05	-3.18E-04
11	0.07	6.38E-04	5.62E-04	7.54E-05	-5.30E-04
12	0.00	6.38E-04	6.38E-04	-6.38E-04	-8.13E-04
13	0.78	6.38E-04	0	0	-1.06E-04

Based on the principles developed by Exner (1920), we expect positive changes in sediment transport to be associated with stable or progradational regions and negative changes in sediment transport to be associated with erosive regions (Equation 14). The congruence of the calculated and the observed change in sediment transport rates is apparent for most, but not all, of the regions, and affirms the idea that calculating longshore sediment transport rates without considering LWD concentration produces erroneous results (Figure 23).

5. Discussion

After the old Brazos delta was abandoned in 1929, water and LWD were no longer actively delivered to the delta. However, we anticipate that prior to the abandonment, the delta should have maintained accumulations of LWD naturally derived from the river, similar to the observations from the modern delta system. However, after the diversion, the remaining LWD on the old delta was likely removed via a combination of longshore transport, decomposition, and anthropogenic collection. For example, the old delta could have been mined of LWD for use as an inexpensive fuel source during the onset of the Great Depression (i.e., 1929 through early 1930's). Unlike the old delta, the modern delta receives continuous delivery of LWD, as evidenced by field observations.

Here we link numerical modeling and field studies of the Brazos River delta to evaluate the influence of LWD on this coastal system. Using the Komar delta model, we establish that similar sediment transport characteristic, i.e., diffusivity, cannot be used to capture the time variation of the old and modern delta systems, despite both the similar sediment volume of the deltas, and wave climate of the Gulf of Mexico. This implies that there is an additional control on the modern system that is not found for the old system, and here we report this to be LWD. The emplacement of LWD results in an approximate 10-fold decrease in sediment transport efficiency for the modern delta (Figure 16). Field observations of the modern delta reveal that regions possessing a volumetric concentration of LWD higher than 0.4 prograde rather than erode over the time frame from 2010 to 2014 (Figure 20). Alternatively, in the absence of LWD, we predict an increase in sediment transport by an order of magnitude. This reveals a first-order positive correlation between shoreline movement and LWD concentration.

The CERC formula is currently one of the most utilized models for calculating sediment transport along a coastline, but is often inaccurate because the formula is highly sensitive to

wave break angles (Figure 22). For the Brazos delta system, the CERC formula overestimates sediment transport but is nevertheless correlative to observations of changes in sediment transport as measured from aerial photographs (Figure 23). We observe that the CERC formula captures the trend of the highly erosive regions that also coincide with little LWD, thus supporting the hypothesis that delta properties such as the presence of LWD at the shoreface provide morphological stability to the delta.

Using the relationships developed for examining LWD, we calculate that for a standard breaking wave boundary stress equal to 13 Pa, regions possessing LWD concentration >0.4 have little erosion, because the form drag produced by the LWD is sufficient to attenuate boundary stress below the threshold of sediment mobility for the median grain diameter of the Brazos River delta. Therefore, theoretically speaking, there should be no sediment transport in local regions with LWD concentrations greater than 0.4. This is congruent with our field study where we observe prograding rather than eroding regions that transition at a LWD concentration at a threshold of 0.4 (Figure 20).

Calculating sediment transport rates using mechanistic sediment transport models produces quantitatively similar results, whereby calculated changes in sediment transport rates are consistent with values calculated via aerial photographs (Figure 23). For some regions, the sediment transport models produce large spatial changes in sediment transport, as a result of the significant increase in form drag due to locally elevated LWD concentration. Therefore, for some regions, significant aggradation is predicted, however this is not observed based on field observations or from using the CERC formula (Equation 1; Figure 23). This discrepancy could arise because the sediment eroded from regions with low LWD concentration may be displaced over a distance longer than is estimated by our calculated region-to-region transfer of sediment

(i.e., greater than 500 m). As for the CERC estimates, a low breaking wave angle could translate to relatively low estimated sediment transport rates (e.g., Equation 1). Overall, by increasing the concentration of LWD, positive divergences in sediment transport coincide stable and/or prograding shoreline conditions (Figure 23).

These analyses – a delta model, a energetics-based model, and a mechanistic sediment transport model – show that LWD on the Brazos River delta is an important component for preserving the morphology of this coastal system over time scales of years to decades. The methods utilized in this study therefore point to the importance of considering LWD concentrations when calculating longshore sediment transport rates for other coastal systems. The role is quite clear: LWD decreases the longshore sediment transport rate by attenuating the wave energy, thereby reducing sediment mobility and erosion along the shoreface. This is particularly true for the Brazos delta. In this special case that considers a classic wave-dominated delta, the river system may only infrequently disperse sediment to the coastline, so that for prolonged drought periods (many years), when little sediment is fluxed to the shoreface, wave energy should produce significant erosion in the absence of LWD. This is hypothesized to have been the situation for the old Brazos delta: that upon removal of the fluvial wood source, the old delta was eroded quickly in 11 years. We suggest that the removal of LWD from the old delta could have been associated with anthropogenic activities. For example, 1929 coincides with the onset of the Great Depression, so humans could have harvested LWD from the old Brazos delta for use as a cheap fuel source. This, in turn, could have produced accelerated sediment erosion rates, and the rapid demise and erosion of the old delta. We lean on this hypothesis because, during the course of our field investigations of the modern delta, we encountered many situations whereby the eastern side of the Brazos delta – the side that is accessible to vehicular

traffic and heavily influenced by anthropogenic activity and therefore not investigated in this study – remains prime ground for LWD collection by humans as a fuel source (Figure 24).

This research has important implications for coastal restoration and mitigation efforts. Particularly moving into a future of diminished sediment loads, amplified droughts, and rising sea levels, coastal systems are ever more prone to erosion and destruction. In many environments, engineering measures have been implemented that, to some extent, mimic the role of LWD. Known as tetrapods, concrete blocks are used world-wide in eroding coastal systems in order to attenuate wave energy (Figure 25). Unfortunately, while effective in the short term, these measures often lend to continued erosion because the dense concrete is frequently undercut by wave energy, resulting in the eventual failure of the tetrapods. Alternatively, LWD may serve as a natural and stable buffer to wave climate, because during significant storm surge events, LWD is buoyant and therefore minimizes undercutting, making it an excellent protector for sandy shorefaces during day-to-day wave activity and perhaps even low-intensity storm events. Major ocean storms (e.g., hurricanes) with significant storm surges (i.e., >3 m), will likely float and remove the LWD — but not completely undercut the beach and produce failure, as is often the case with concrete tetrapods. We therefore suggest that, based on this study, LWD is a natural way to protect coastal shorefaces from day-to-day wave and small to moderate storm events. Thus, LWD, by attenuating sediment transport capacity by up to an order of magnitude, has important implications for the long-term stability of coastal regions.

Finally, the Brazos delta has significant importance to the city of Freeport and surrounding regions, because this growing coastal land baffles storm surge and could reduce the negative influence these regions experience as a result of rising sea level ocean storms. In this regard, the Brazos provides a unique opportunity to examine the implications of LWD on

coastlines. Although the long term stability of this region is important in its own right, this project has broader implications that can be applied globally, as LWD is found for many delta systems (e.g., the Yukon, Mahakam, and Colorado (Texas) Rivers; Hartopo, 1991, Coleman et al., 2003), and coastline protection for coastal systems may leverage the effect of LWD to protect against extensive shoreline erosion.

6. Conclusions

This study provides an innovative linkage between a reduction in longshore sediment transport and LWD using a numerical model, field surveys, and analysis based on first-order principles of sediment transport from an energetics formulation. As an end-member wave-dominated delta, observations from the Brazos delta system provide insight into the classification "wave-dominated delta" as a whole, and allow for reevaluation of the delta's key controls on its morphological stability.

The relative stability of the modern Brazos system, compared to the rapidly eroded old system whereby all morphological signature of the delta was removed in less than 11 years upon completion of a engineered river channel diversion, supports the hypothesis that LWD has an integral role in terms of coastal sediment transport, whereby LWD stabilizes delta morphology by muting longshore sediment transport by inducing additional form drag. The reduced longshore sediment transport allows for relative stability during times of reduced river sediment discharge, and ultimately stabilizes the delta.

This project provides the quantitative framework required to evaluate the role of LWD, and therefore could apply to evaluating appropriate coastline mitigation strategies. That said, to fully constrain the effects of LWD on any particular coastal systems, research regarding the wave climate and sediment source and sizes are required. The relationships developed here

nevertheless provide a first-order framework for evaluating the role of LWD for reducing longshore sediment transport and stabilizing coastal morphology.

Bibliography

Abbe, T. (2000). Patterns , Mechanics and Geomorphic Effects of Wood Debris Accumulations in a Forest River System. Doctoral Thesis.

Abbe, T. B., and Montgomery, D. R., (1996), Large woody debris jams, channel hydraulics and habitat formation in large rivers: Regulated rivers: Research and Management, v. 12, p. 201–221.

Alperin LM. Custodians of the Coast: History of the United States Army Engineers at Galveston. Galveston, Tex: Galveston District; 1977.

Anderson, J.B. (2014) Personal Communication.

Angradi, T. R., Schweiger, E. W., Bolgrien, D. W., Ismert, P., & Selle, T. (2004). Bank stabilization, riparian land use and the distribution of large woody debris in a regulated reach of the Upper Missouri River, North Dakota, USA. River Research and Applications, 20(7), 829–846. doi:10.1002/rra.797

Ashida, K. and Michiue, M. (1972). “Study on hydraulic resistance and bedload transport rate in alluvial streams.” Transactions, Japan Society of Civil Engineering, No. 206, 59-64.

Ashton, A. D., and L. Giosan (2011), Wave-angle control of delta evolution, Geophysical Research Letters, 38, L13405, doi:10.1029/2011GL047630.

Assani, A., and F. Petit. (1995). Log-jam effects on bed-load mobility from experiments conducted in a small gravel-bed forest ditch. Catena 25:117-126.

Beddall, M. (2009). Japan's Concrete Coast. http://www.mikesblender.com/tokyo_concretecoast.php

Booth, D.B., Montgomery, D.R., Bethel, J., 1997. Large Woody Debris in Urban Streams of the Pacific Northwest: in Roesner, L.A., ed., Effects of watershed development and management on aquatic ecosystems: Engineering Foundation Conference, Proceedings, Snowbird, Utah, August 4-9, 1996, 178–197.

Cherry, J., & Beschta, R. L. (1989). Coarse woody debris and channel morphology: A flume study. Water Resource Bulletin. 25(5), 1031–1036. doi:10.1111/j.1752-1688.1989.tb05417.x

Coleman, J. M., O. K. Huh, and D. Braud. 2003. Major World Deltas: A Perspective from Space. Research report submitted to NASA.

Dietrich, W. E., and J. D. Smith (1984), Processes controlling the equilibrium bed morphology in river meanders, in River Meandering, edited by C. M. Elliot, pp. 759–769, Am. Soc. of Civ. Eng., New York.

Eamer, J. B. R., & Walker, I. J. (2010). Quantifying sand storage capacity of large woody debris on beaches using LiDAR. Geomorphology, 118(1-2), 33–47. doi:10.1016/j.geomorph.2009.12.006

Exner, F. M. (1920), Zur physik der dünen, Akad. Wiss. Wien Math. Naturwiss. Klasse, 129(2a), 929–952.

Fraticelli, C. M. (2006). Climate Forcing in a Wave-Dominated Delta: The Effects of Drought-Flood Cycles on Delta Progradation. Journal of Sedimentary Research, 76(9), 1067–1076. doi:10.2110/jsr.2006.097

Gibeaut, J. C., White, W. A., Hepner, T., Gutierrez, R., & Tremblay, T. A. (2000). Texas Shoreline Change Project Gulf of Mexico Shoreline Change from the Brazos River to Pass Cavallo, (October).

Gippel, C.J., I.C. O'Neill, B.L., Finlayson & I. Schnatz, (1996). Hydraulic guidelines for the re-introduction and management of large woody debris in degraded lowland rivers. Regulated Rivers: Research and Management, vol. 12, 223-236.

Gurnell, A. M., Pie, H., & Northwest, P. (2002). Large wood and fluvial processes, 601–619.

Hamilton, M. D. (1995). Detailed Facies Analysis of the Brazos Wave Dominated Delta Freeport Texas.

Hartopo. 1991. The effect of raft removal and dam construction on the Lower Colorado River, Texas. Unpublished M.S. Thesis, Texas A & M University.

Heathfield, D. K., & Walker, I. J. (2011). Analysis of coastal dune dynamics, shoreline position, and large woody debris at Wickaninnish Bay, Pacific Rim National Park, British Columbia. Canadian Journal of Earth Sciences, 48(July), 1185–1198. doi:10.1139/e11-043

Heede, B. (1985). Interactions between streamside vegetation and stream dynamics. Riparian Ecosystems And Their Management: Reconciling Conflicting Uses. First North American Riparian Conference, April 16-18, 1985, Tucson, Arizona, 54–58.

Hygelund, B., & Manga, M. (2003). Field measurements of drag coefficients for model large woody debris, Geomorphology. 51, 175–185.

Inman, D.L., and Bagnold, R.A. (1963). Littoral processes. The Sea.vol. 3, M.N. Hill, ed., Interscience, New York, 529-553.

Keel, J. (2014). The Brazos River Authority, An Audit Report on the Brazos River Authority. State Auditor's Office Report Number 14.

Komar, P. D. (1971). The mechanics of sand transport on beaches. Journal of Geophysical Research, 76(3), 713. doi:10.1029/JC076i003p00713

Komar, P. D. (1973). Computer Models of Delta Growth due to Sediment Input Computer Models of Delta Growth due to Sediment Input from Rivers and Longshore Transport. doi:10.1130/0016-7606(1973)84<2217

Komar, P. D., & Inman, D. L. (1970). Longshore Sand Transport on Beaches in and near and compute and spectra [Koontz and p are . respectively the sand and tools began in 1966 . In a preliminary report for pore space and can be taken It is Inman verified that the longshore advantageous to ex, 75(30), 5914–5927.

Manga, M., & Kirchner, J. W. (2000). Stress partitioning in streams by large woody debris, Water Resources Research, vol. 36, no. 8, 2373–2379.

Montgomery, D. R., & Piégay, H. (2003). Wood in rivers: interactions with channel morphology and processes. Geomorphology, 51(1-3), 1–5. doi:10.1016/S0169-555X(02)00322-7

Nelson, J. M., and J. D. Smith (1989), Flow in meandering channels with natural topography, in River Meandering, Water Res. Monogr. Ser., vol. 12, edited by S. Ikeda and G. Parker, pp. 69–102, AGU, Washington, D. C.

Phillips, J.D., (2006). Field data collection in support of geomorphic classification of the lower Brazos and Navasota Rivers. Texas Water Development Board, 100 p.

Rodriguez, A. B., Hamilton, M. D., & Anderson, J. B. (2000). Facies and evolution of the modern Brazos delta , Texas : wave versus flood influence.

Seelam, JK and Baldock, Thomas E. (2009). Direct bed shear stress measurements under solitary tsunami-type waves and breaking tsunami wave fronts. In: M. Mizuguchi and S. Sato, PROCEEDINGS OF COASTAL DYNAMICS 2009. 6th International Conference on Coastal Dynamics, Tokyo JAPAN, (U102-U103). SEP 07-11, 2009.

Seelig, W.N. and Sorensen, R.M., (1973), Investigation of shoreline changes at Sargent Beach, Texas: Texas A&M University Sea Grant, TAMU-SG-73-212, COE-169, 153 p.

Shields Jr., F. and Gippel, C. (1995). ”Prediction of Effects of Woody Debris Removal on Flow Resistance.” J. Hydraul. Eng., 121(4), 341–354.

Smith, R. D., Sidle, R. C., Porter, P. E., & Noel, J. R. (1993). Effects of experimental removal of woody debris on the channel morphology of a forest, gravel-bed stream. Journal of Hydrology, 152(1-4), 153–178. doi:10.1016/0022-1694(93)90144-X

Strom, K. and Rouhnia, M. (2013). Suspended Sediment Sampling and Annual Sediment Yield on the Lower Brazos River. Texas Water Development Board Report.

USACE. (1984) US Army Corp of Engineers Shoreline Protection Manual. Vicksburg, MS.

Wallace, D. J., Anderson, J. B., & Fernández, R. a. (2010). Transgressive Ravinement versus Depth of Closure: A Geological Perspective from the Upper Texas Coast. Journal of Coastal Research, 26(6), 1057–1067. doi:10.2112/JCOASTRES-D-10-00034.1

Watson, R. L. (2003). Severe Beach Erosion at Surfside, Texas Caused by Engineering Modifications to the Coast and Rivers. Unpublished Report Prepared for Russell Clinton of Surfside, Texas, 78373(361), 1–34. Retrieved from http://texascoastgeology.com/papers/surfside.pdf\nhttp://coastal.tamug.edu/AM/TGLOProjects/SevereBeachErosionatSurfsideTXCausedbyEngineeringMo.PDF

Wiberg, P. and Dungan Smith, J. (1989). ”Model for Calculating Bed Load Transport of Sediment.” Journal of Hydraulic Engineering, 115(1), 101–123.

Wilson, K. C. (1966). Bed-load transport at high shear stress. Journal of the Hydraulics Division, 92(6), 49-59.

Zelo, I., & Shipman, H., Brennan J. (2000). Alternative Bank Protection Methods for Puget Sound Shorelines. Washington State Department of Ecology publication #00-06-012.

Figures

Figure 1: Map of the Brazos River Basin modified from Rodriguez et. al. (2000). The basin encompasses a large area that spans from eastern New Mexico to south east Texas

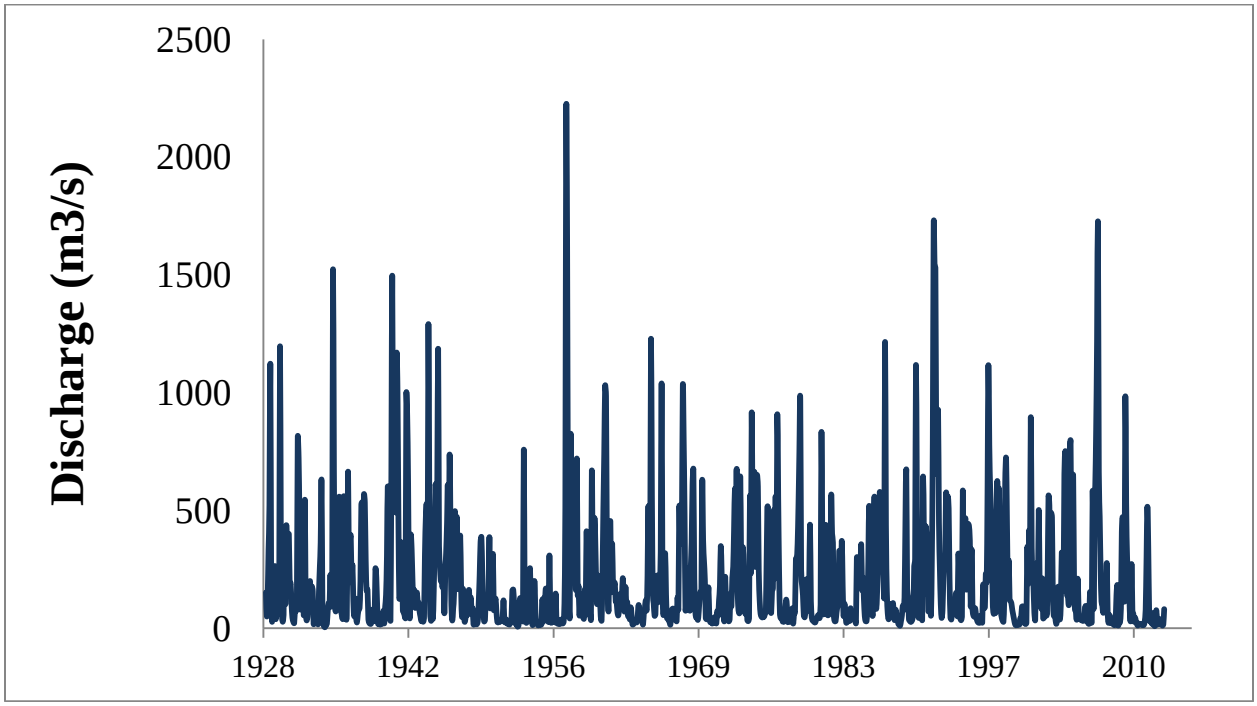

Figure 2: Brazos River water discharge from 1929 to 2013 based on data from Richmond USGS data station on the Lower Brazos, 80 km from the river mouth.

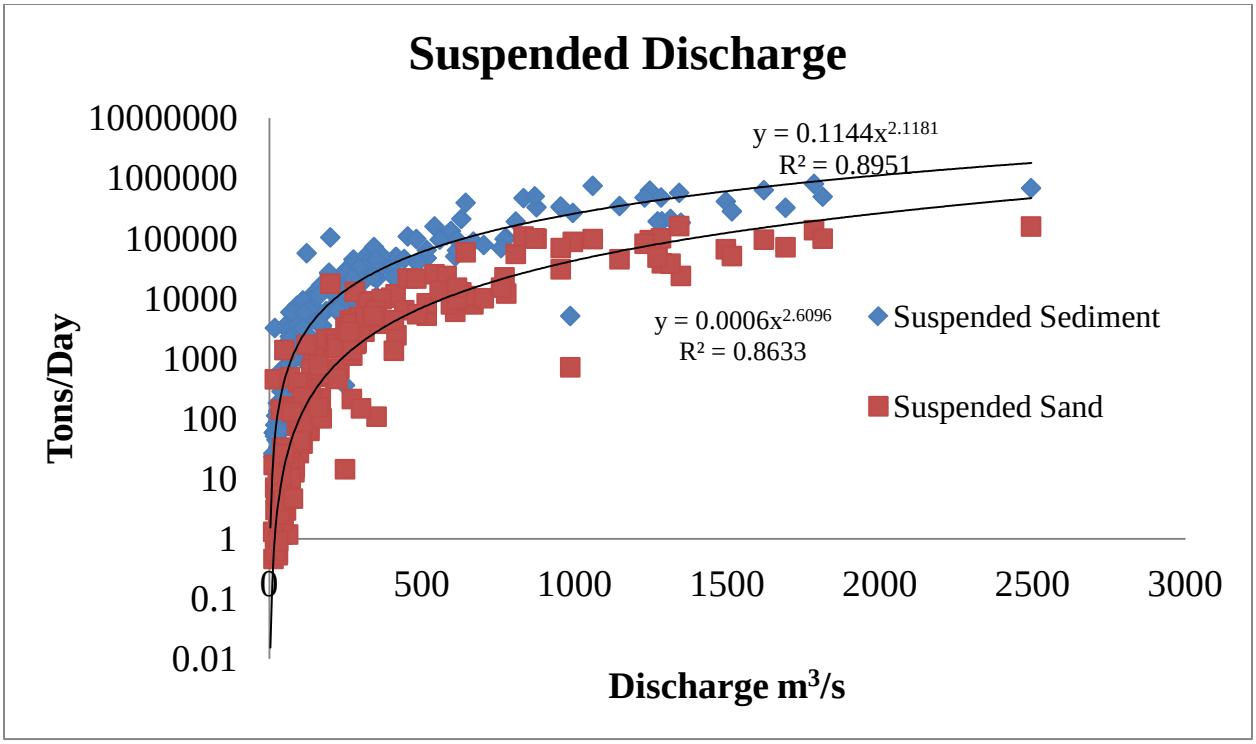

Figure 3: Suspended sediment (mud and sand) and suspended sand discharge and water discharge, as measured from the Richmond station. Both vary non-linearly with respect to water discharge. The exponential function was chosen so to minimize the residuals.

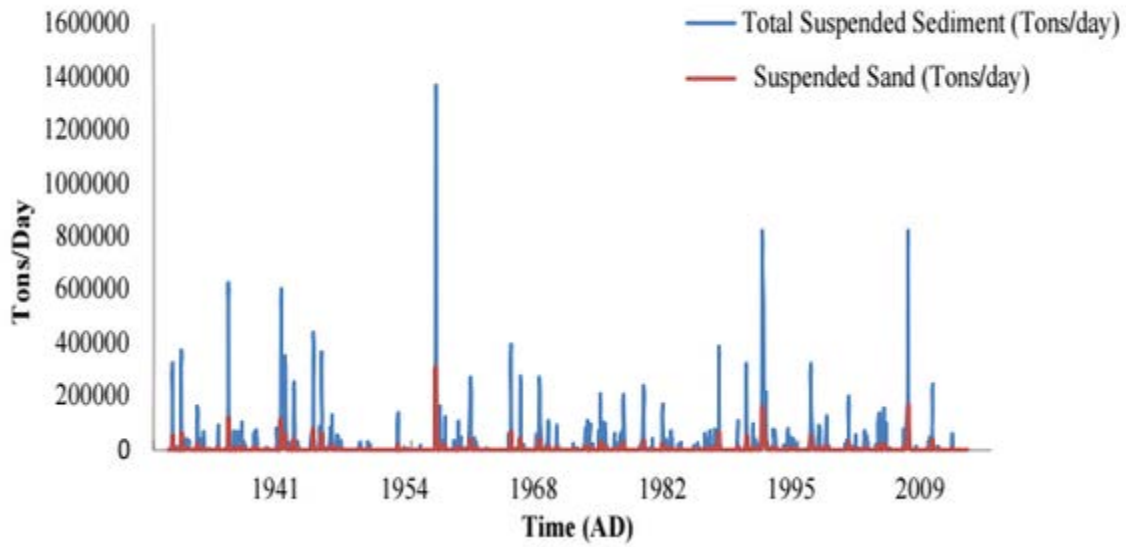

Figure 4: Suspended sediment (mud and sand) and suspended sand discharge over time. Both vary non-linearly with respect to water discharge, thereby producing accentuated peaks during flood conditions.

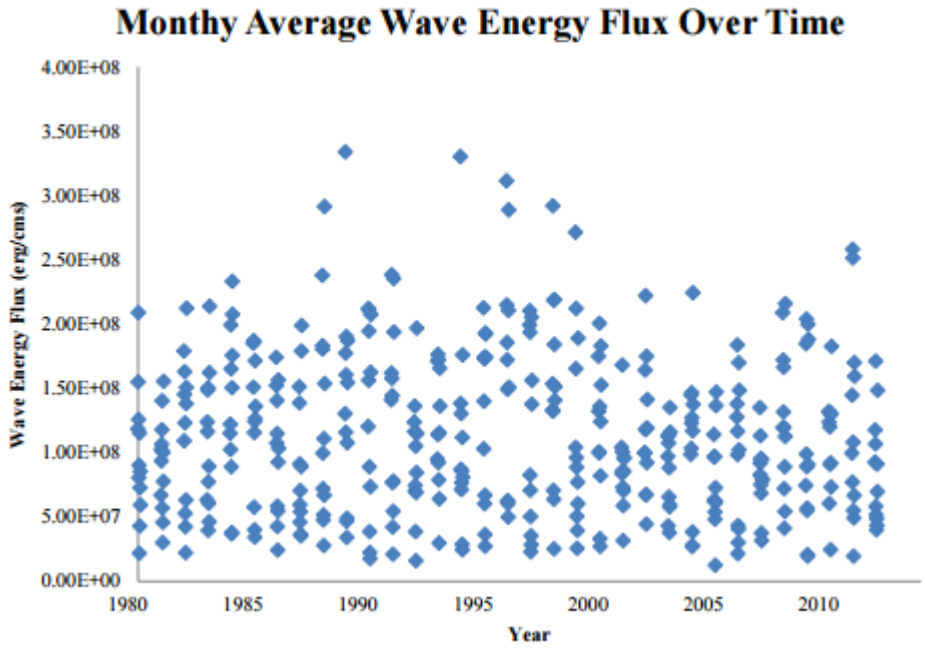

Figure 5: Wave energy flux data for the period of 1980 to 2013, as calculated based on data from USACE Station WIS 73064, 24 km from the coast.

Figure 6: Photos taken along the Brazos River Delta shoreline demonstrating the abundance of large LWD.

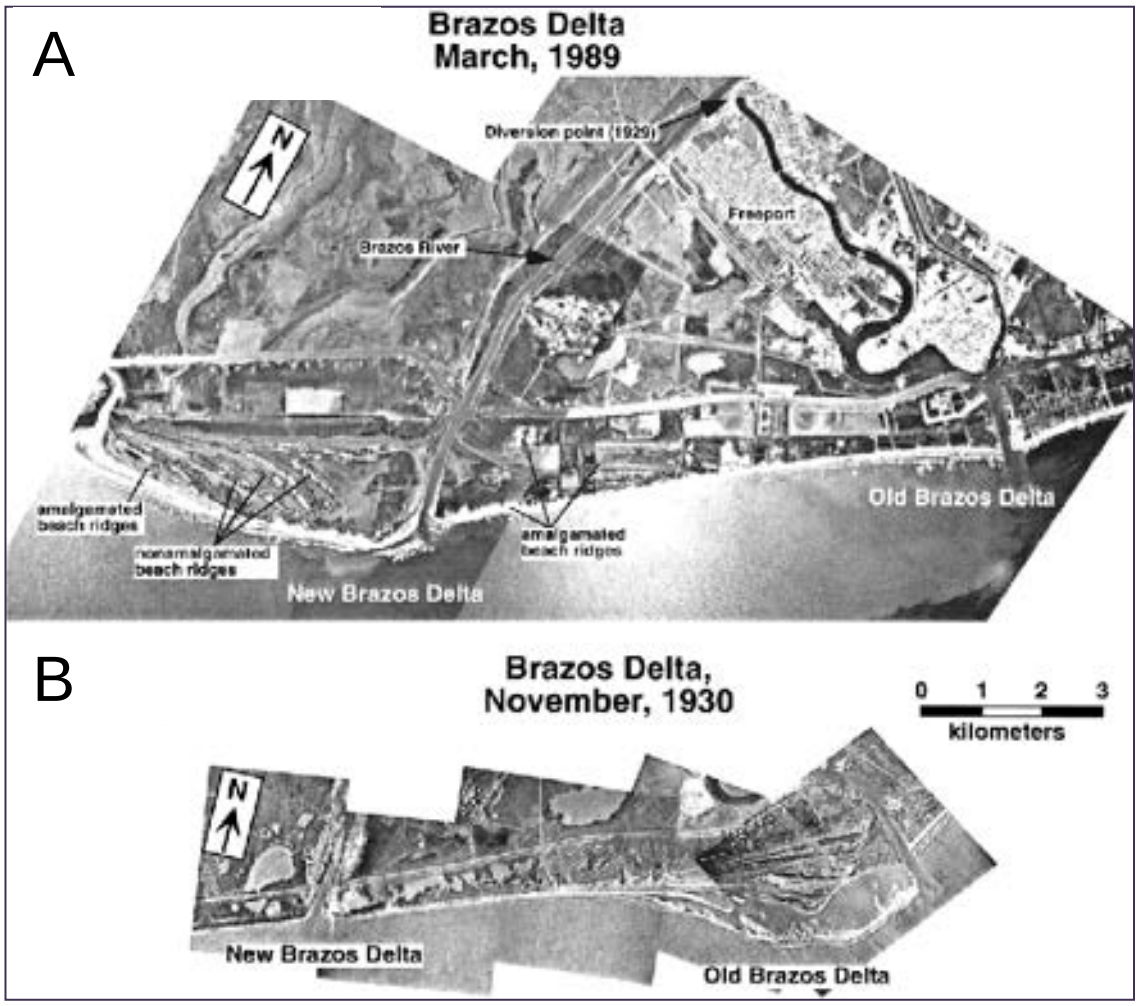

Figure 7: Aerial photographs of the modern (A) and old (B) Brazos River deltas (Rodriguez et al., 2000)

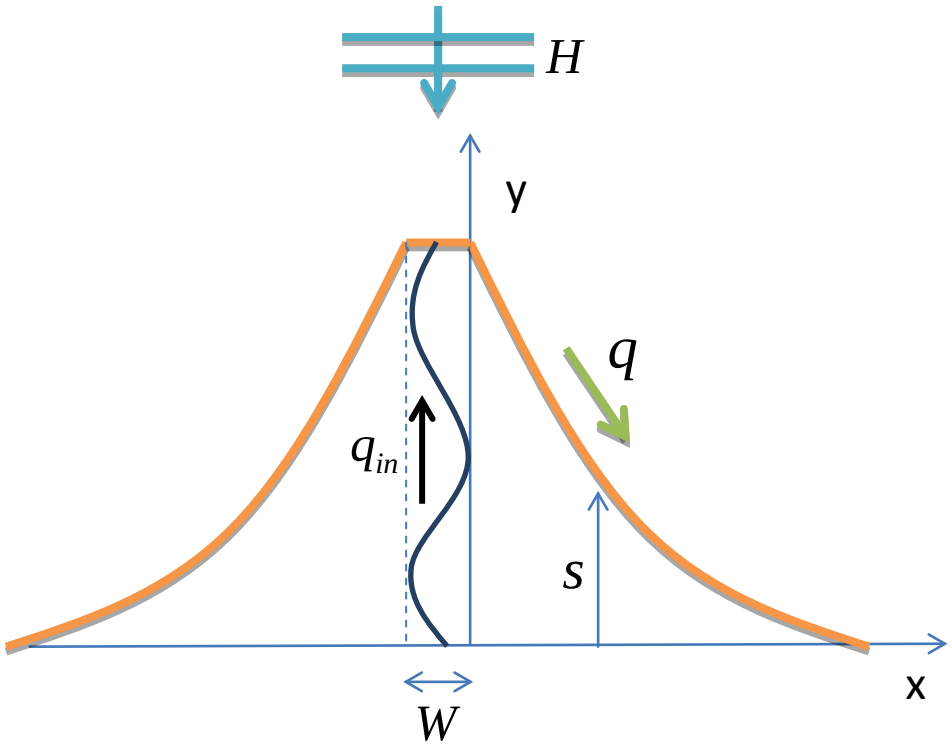

Figure 8: Planform view of the symmetric delta model used here, where q_{in} is constrained based on monthly sediment discharge data from the Richmond USGS station, W is set at 250 m the observed river mouth width. H is the wave height, directed perpendicular to the river mouth. S is defined as the position of the shoreline (y) from the datum at any point along the datum, or x-axis. q_a or longshore sediment flux is determined as a function of the diffusivity and slope of the shoreline.

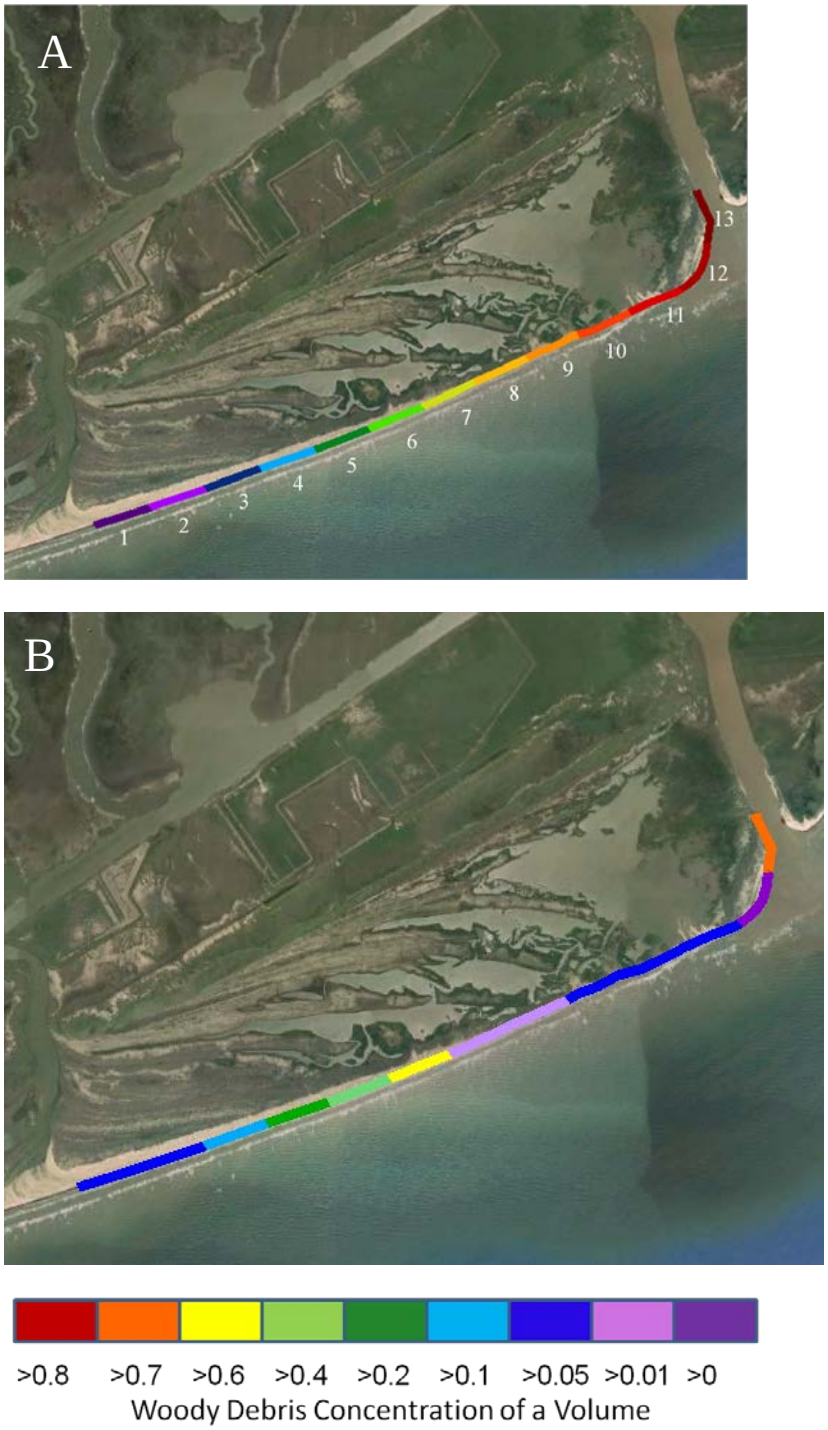

Figure 9: Map showing the 13 discrete Brazos River delta regions (A, shaded with increasingly warmer colors from region 1 to region 13), each 500 m in length, the midpoints of which are used for shoreline sediment transport analysis (See Table 1). B is a map showing the LWD concentration of each region (B), where regions are shaded indicating LWD concentration.

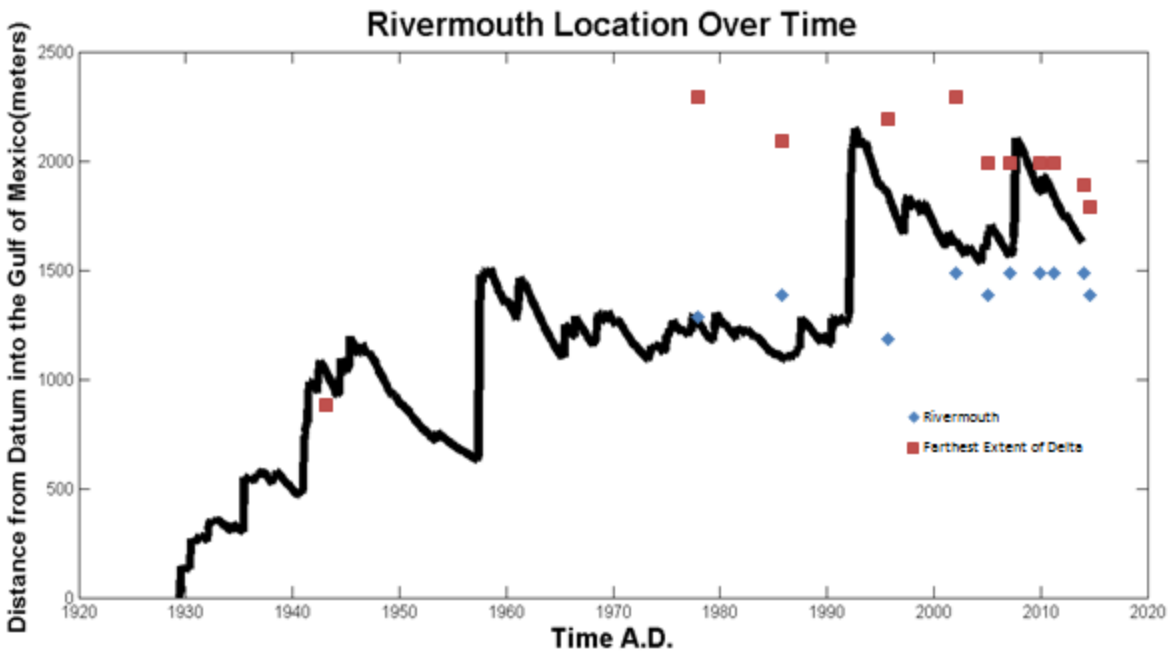

Figure 10: The river mouth location and time, where the dark solid line represents the model results, overlain with the historical river mouth locations and farthest extents of the delta, based on aerial photographs.

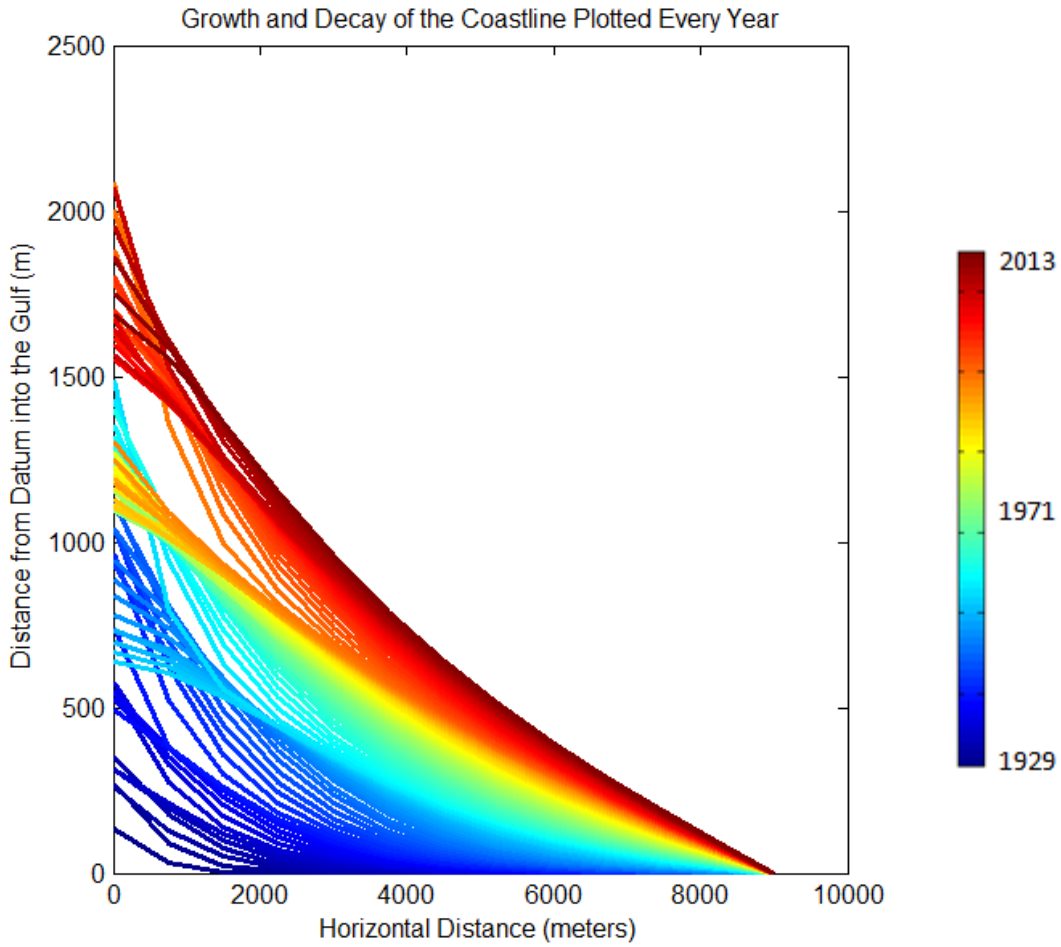

Figure 11: Model run for delta growth, for the years 1929 to 2013, developing into a constant basin depth. Here, a diffusivity value of γ=22500 is used to capture both the basinward extent and lateral development of the modern Brazos delta, where the model is tuned using the measured development history of the delta.

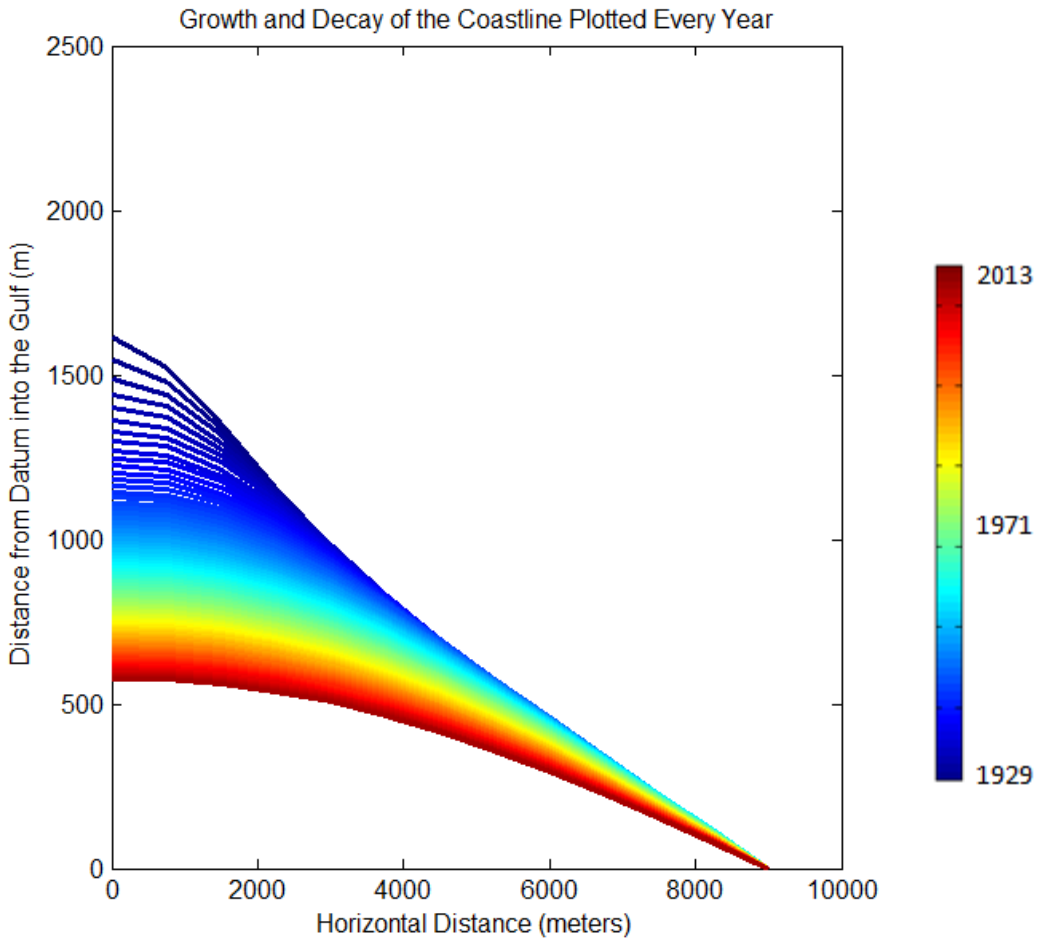

Figure 12: Model run for the erosion of the old Brazos delta, using the same diffusivity value as Fig. 11 (i.e., γ=22500). Note that the delta does not come close to eroding in the eleven-year time frame as was measured. In fact, this diffusivity value renders the delta in place in the year 2013, despite cutoff of water and sediment.

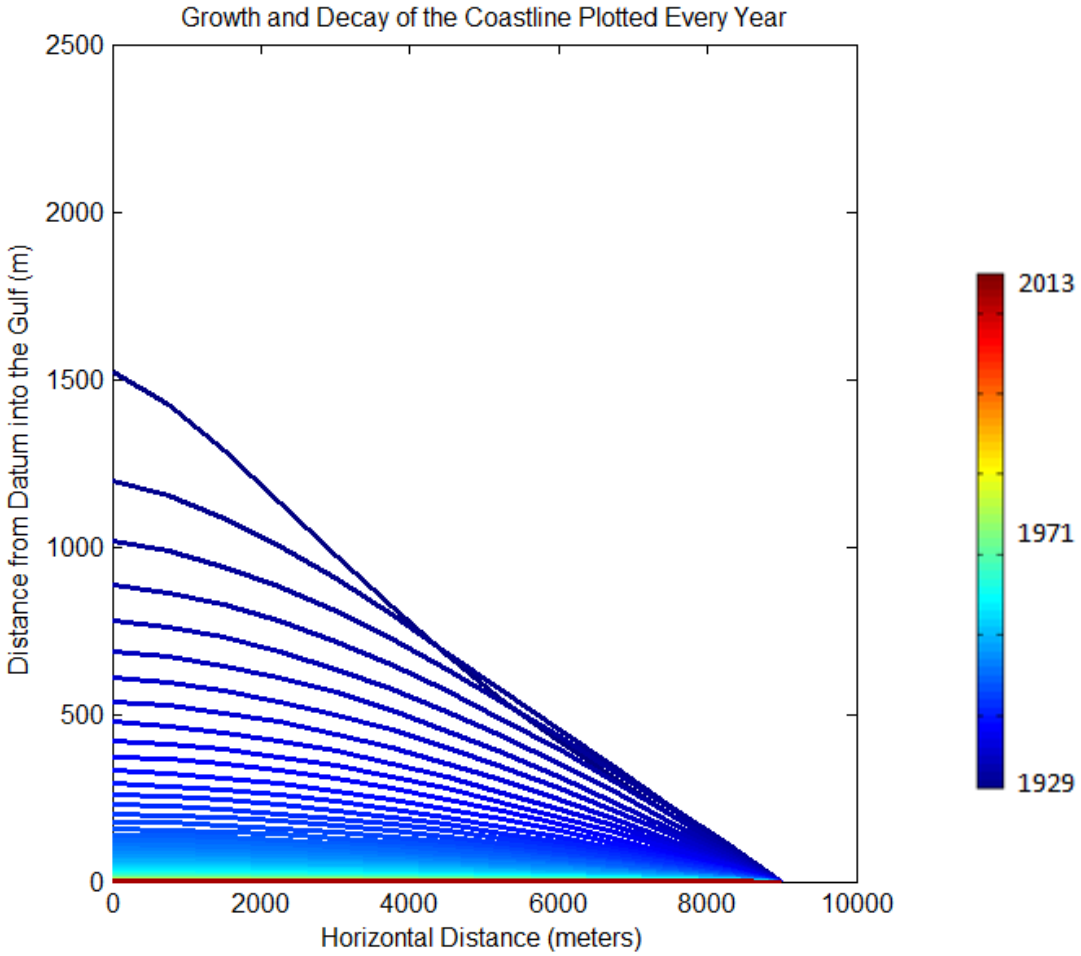

Figure 13: Model run to describe erosion of the old Brazos delta as constrained by complete removal of the delta in the eleven-year time frame, as was observed for 1929-1940. To appropriately capture erosion of the old Brazos delta, a Diffusivity value of γ=225,000 is required.

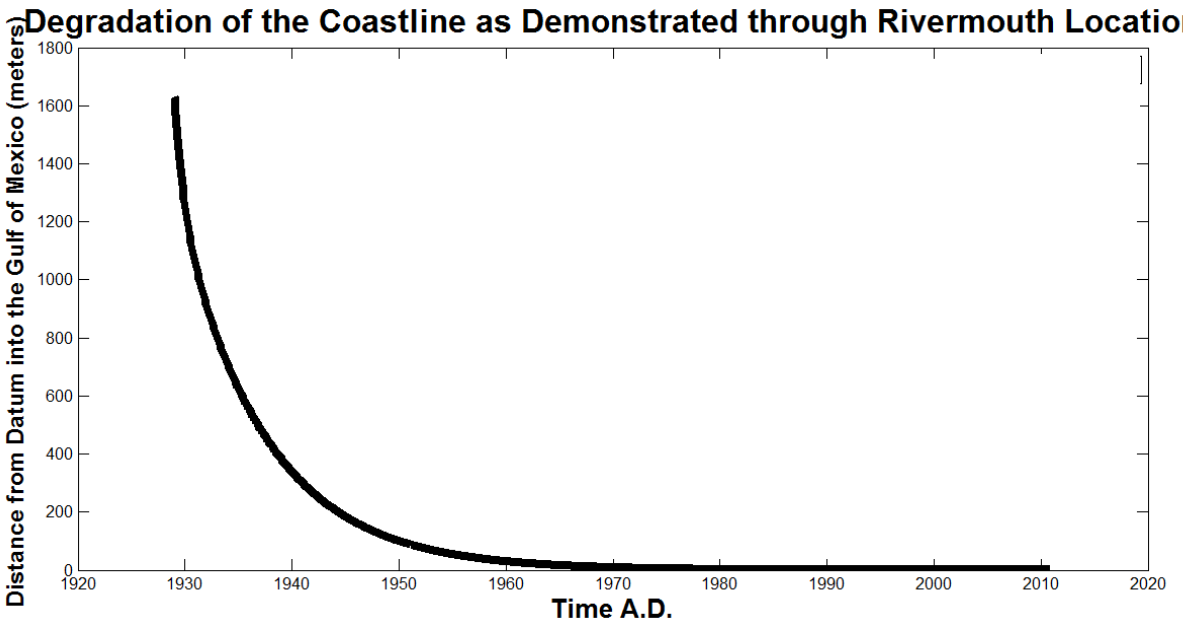

Figure 14: River mouth location over time as modeled for the old Brazos delta, using a diffusivity value of γ =225,000.

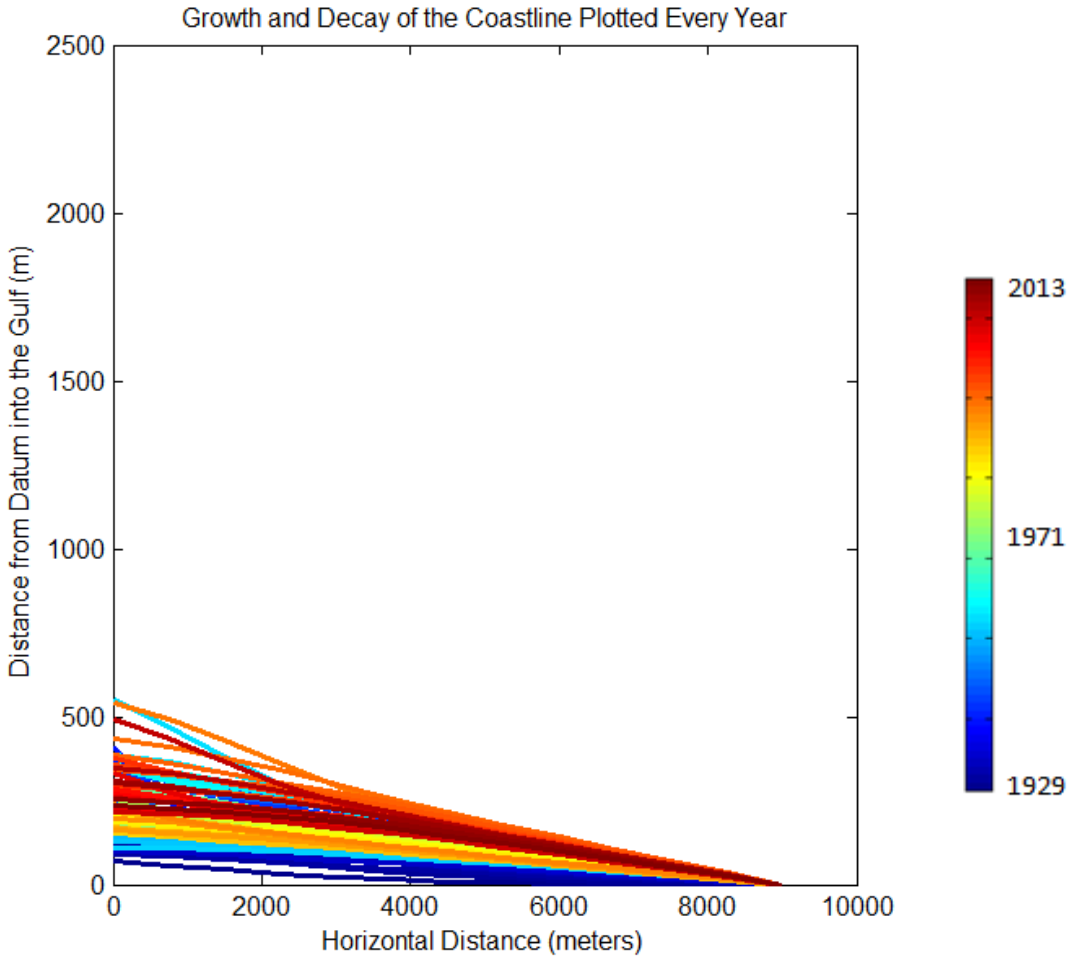

Figure 15: Model run that attempts to grow the modern Brazos delta using a diffusivity value of γ=225,000. It is clear based on these results that the diffusivity needed to erode the old Brazos delta in the appropriate time frame (eleven years) is too high to allow for observed development of the modern Brazos delta.

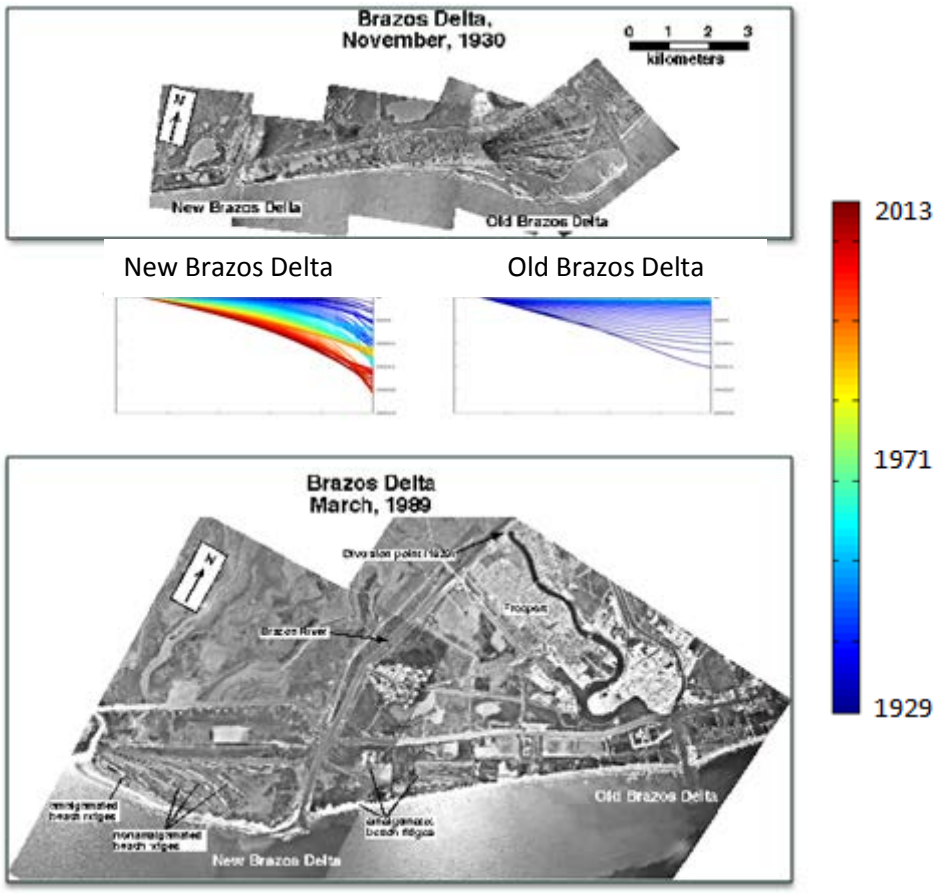

Figure 16: Comparing the models for erosion of the old Brazos delta, and growth of the new Brazos delta, to photographs of the region. Note that the two diffusivity values are tuned based on these photographs, i.e., 22,500 for growth of the modern delta, and 225,000 for destruction of the old delta.

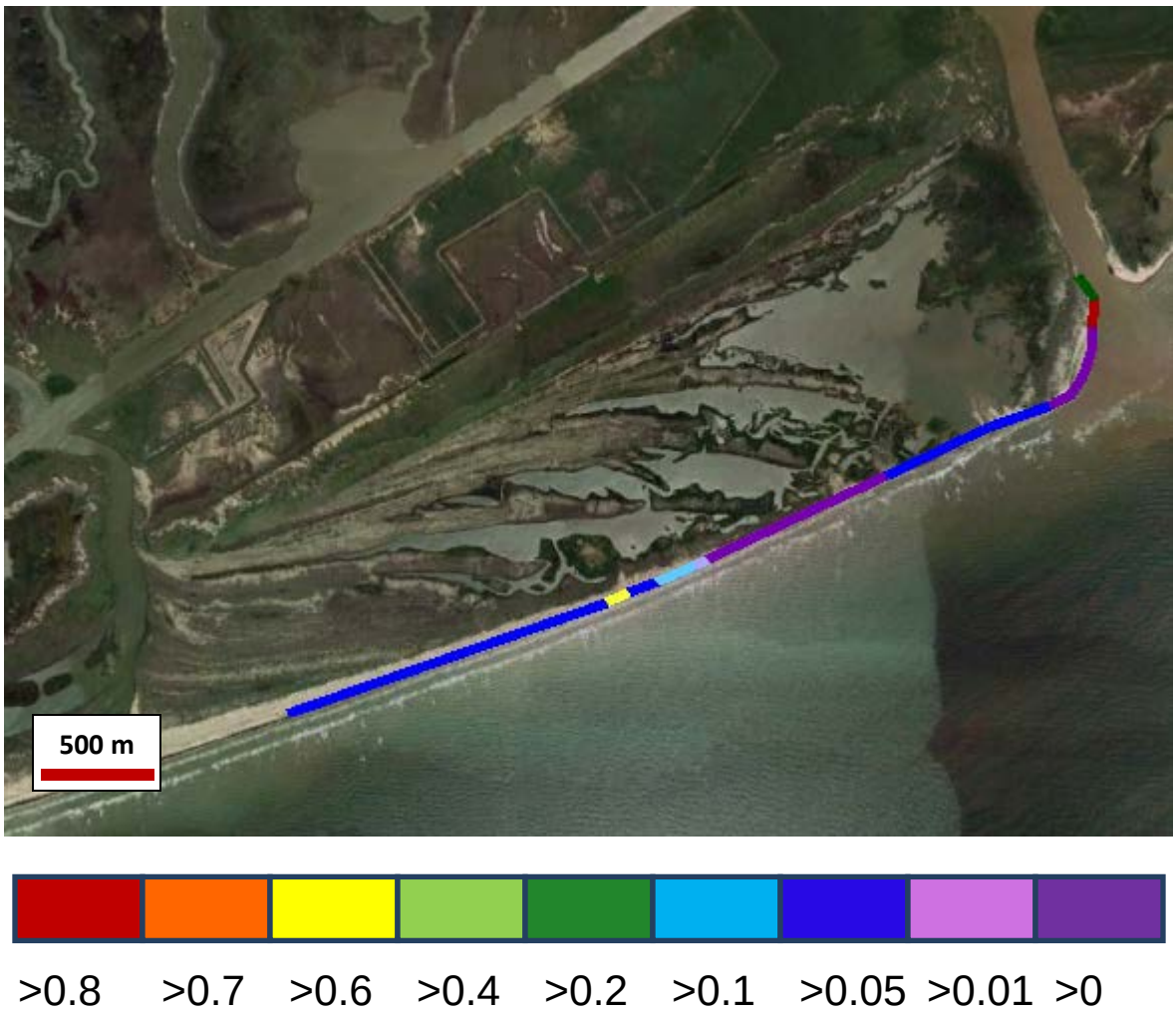

Figure 17: LWD concentrations along the Brazos delta shoreface based on surveys conducted during February, 2015, where breaks in color indicate a new survey site. Concentration is calculated by volume of LWD within a control volume of the shoreface. Warm colors are regions of higher LWD concentration while cool colors have lower concentrations of LWD.

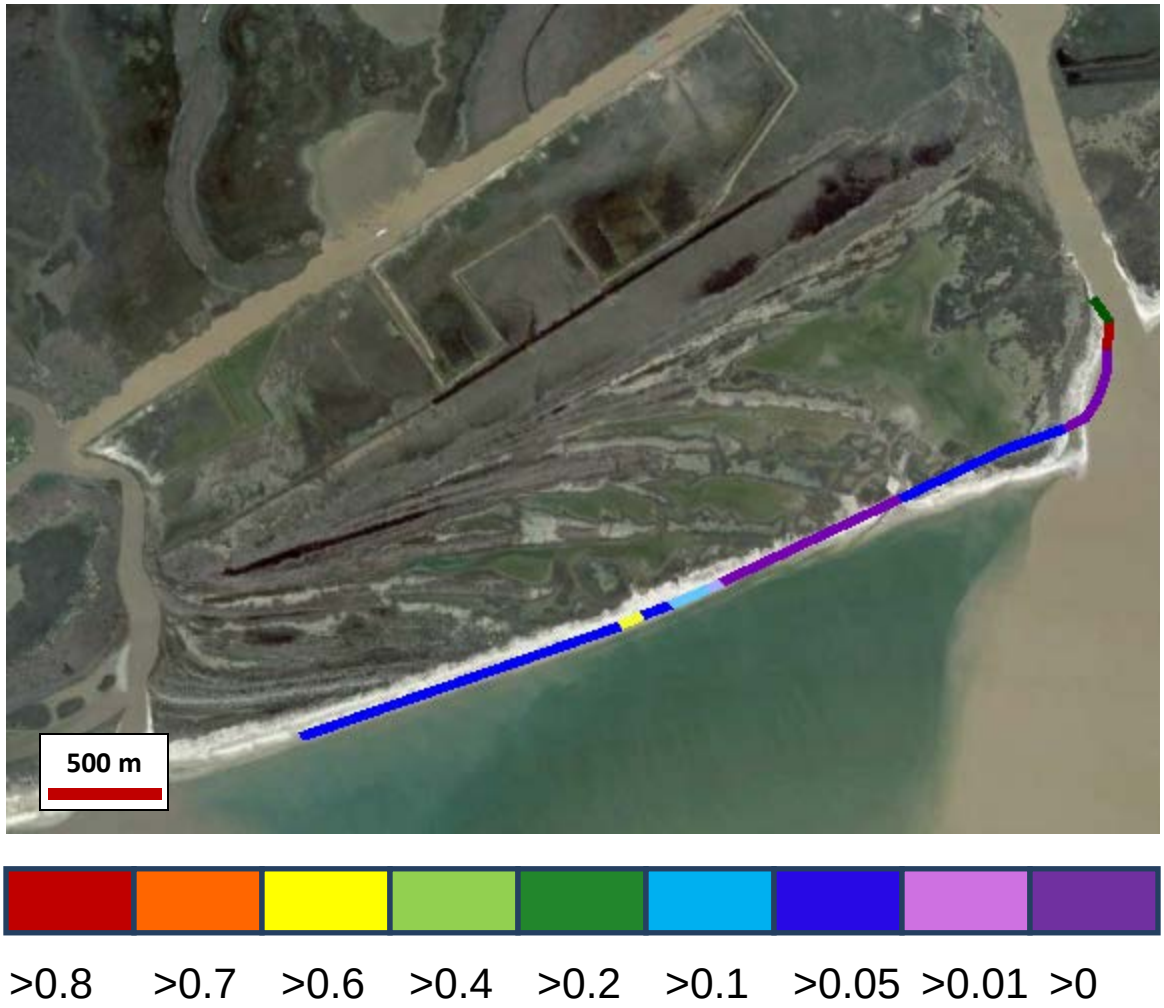

Figure 18: Google Earth image from 2010, with the 2015 shoreline superimposed based on LWD concentration. Note the significant region of erosion near the eastern side of the delta, where LWD concentration is > 0.01. Here, erosion over the five-year period is approximately 150 m.

Figure 19: Shoreface picture taken in 2015 near the eastern side of the Brazos delta, where approximately 150 m of shoreface was eroded, thus exposing back-barrier flora and fauna at the shoreface, including marsh reeds and oysters, amongst mud deposits.

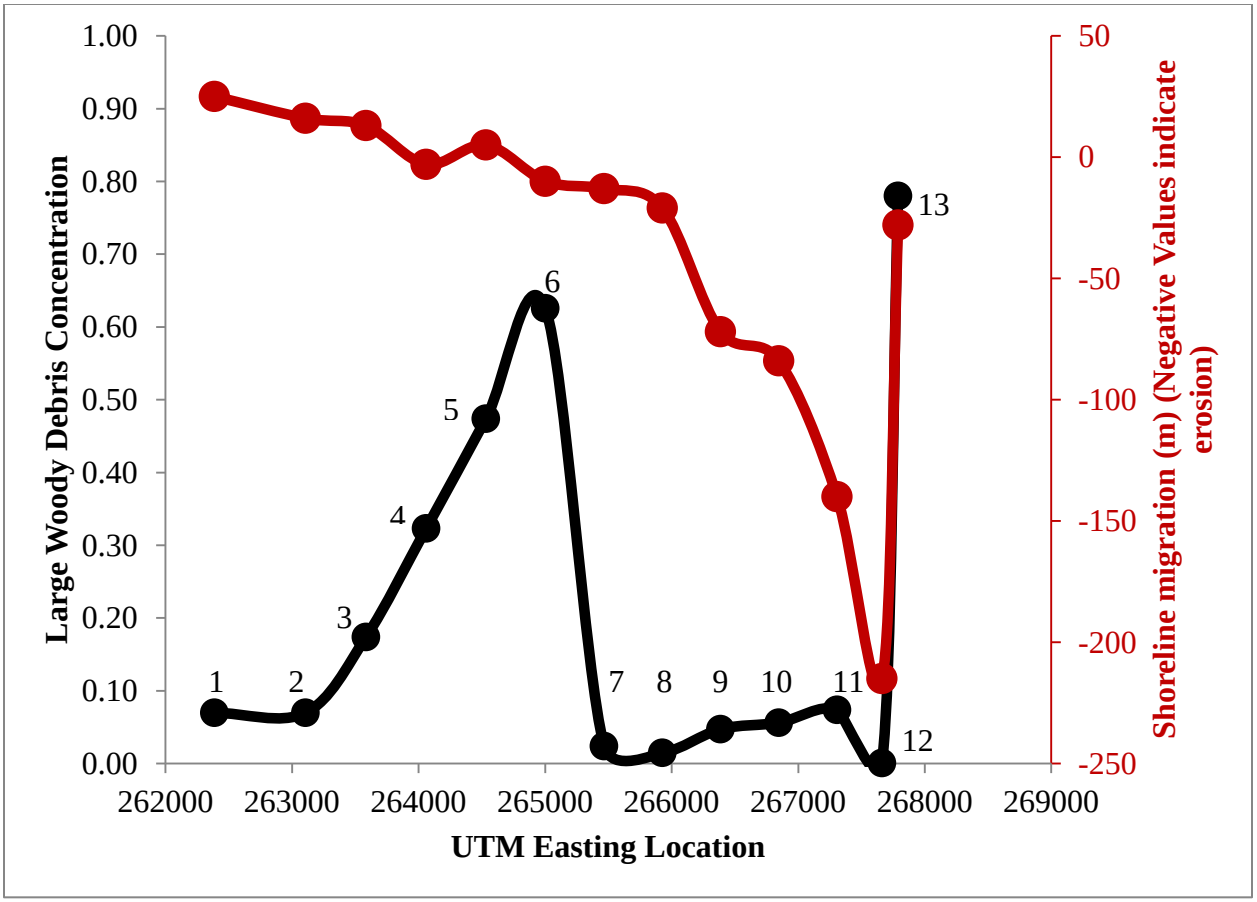

Figure 20: Large woody debris (LWD) concentrations mapped to shoreline location, where the midpoint of each region is noted with respect to its UTM location (black line). Also shown are the measured shoreline movements for each region, based on the difference between the 2010 and 2014 aerial photographs (red line; negative values indicate erosion. Transport direction is west (left in the figure).There is a general trend where lower LWD concentration coincides with regions of significant erosion. These eroded regions may act as a significant source of sediment being delivered down-drift.

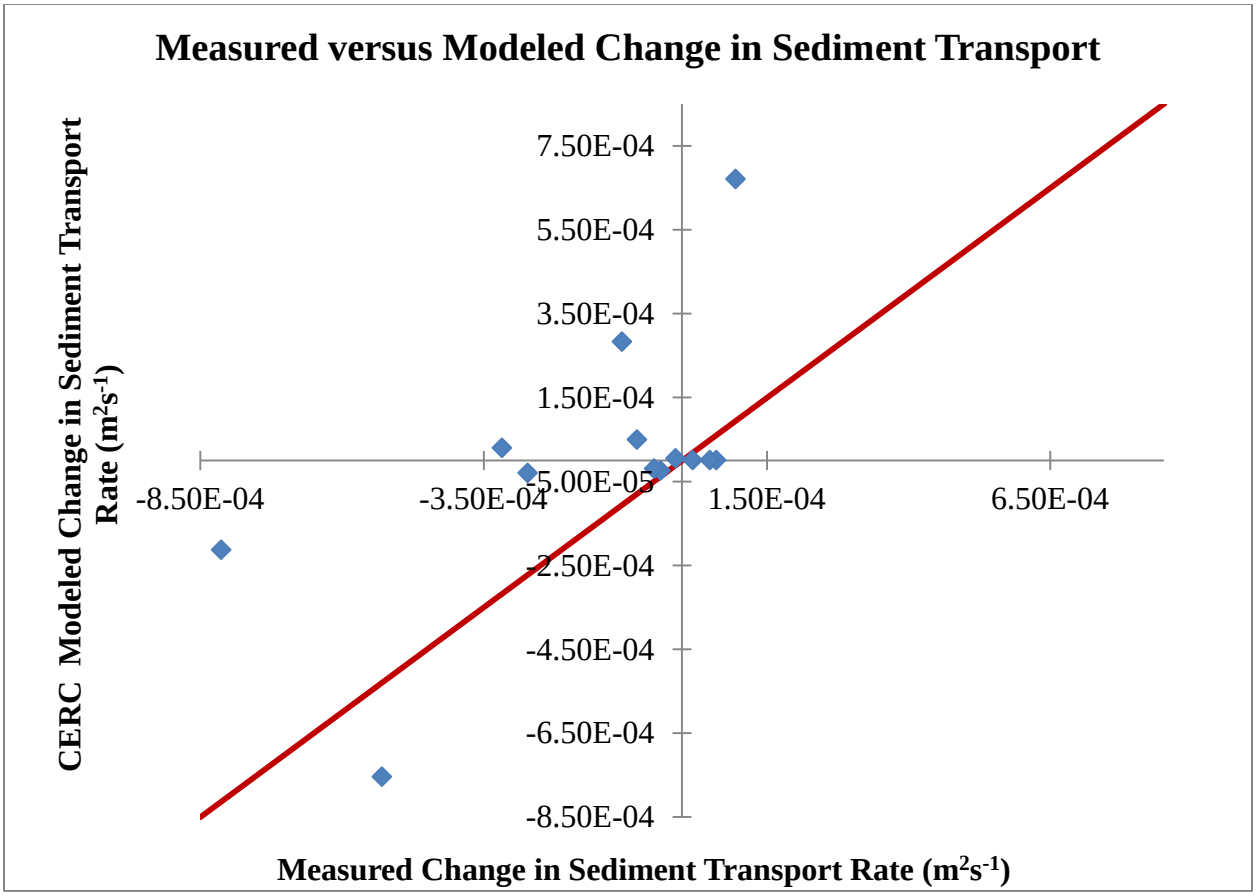

Figure 21: Measured change in sediment transport rates (from 2010-2014 aerial photographs) are compared against modeled change in sediment transport rates, using the CERC model for sediment transport. The red line indicates a 1 to 1 ratio.

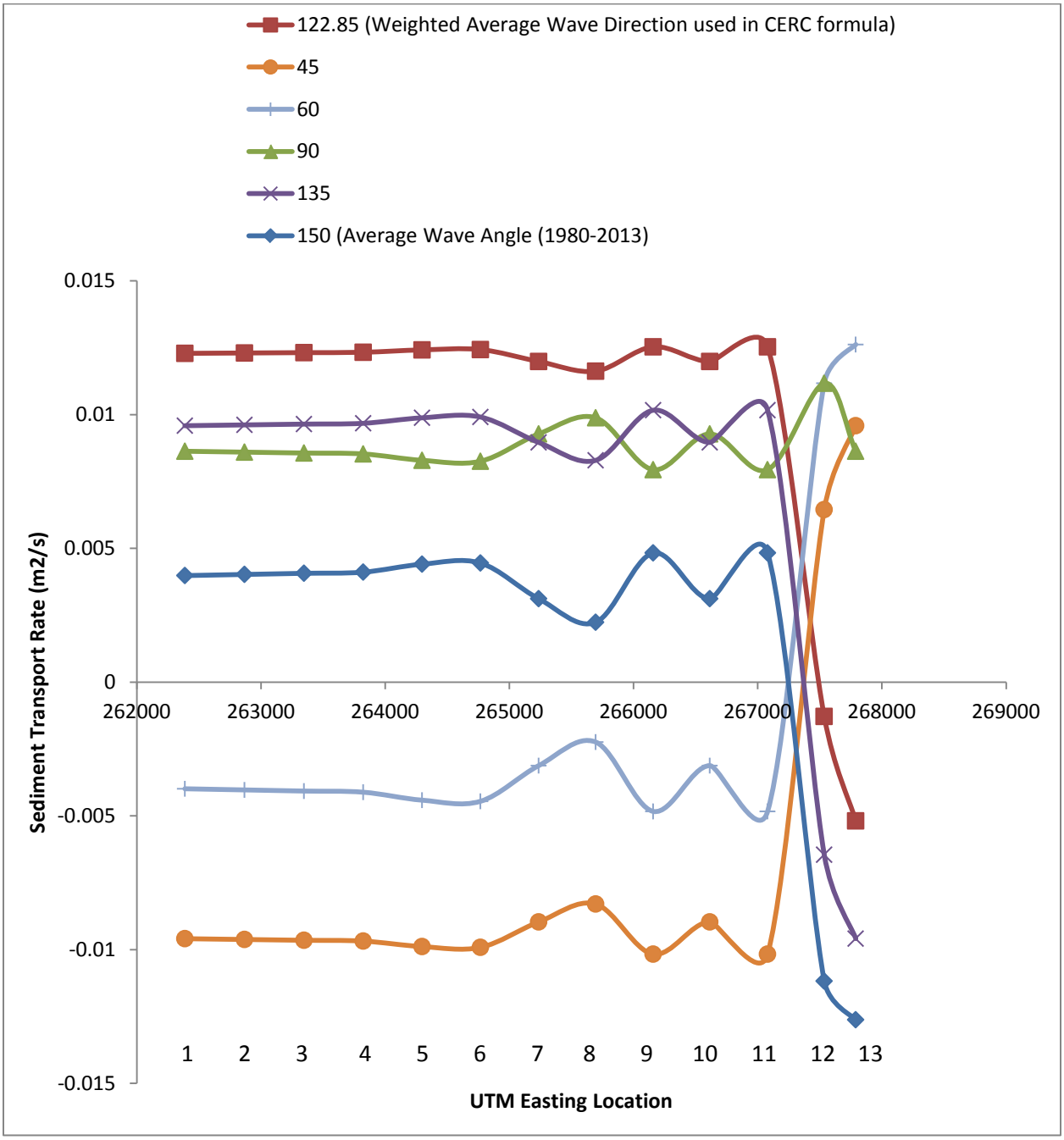

Figure 22: Sensitivity of the CERC formula for predicting shoreface sediment transport, based on different wave break directions. Sediment transport is measured for each region (bottom label) and plotted with its UTM Easting location. Modifying the angle of the wave break significantly alters the modeled rates of sediment transport.

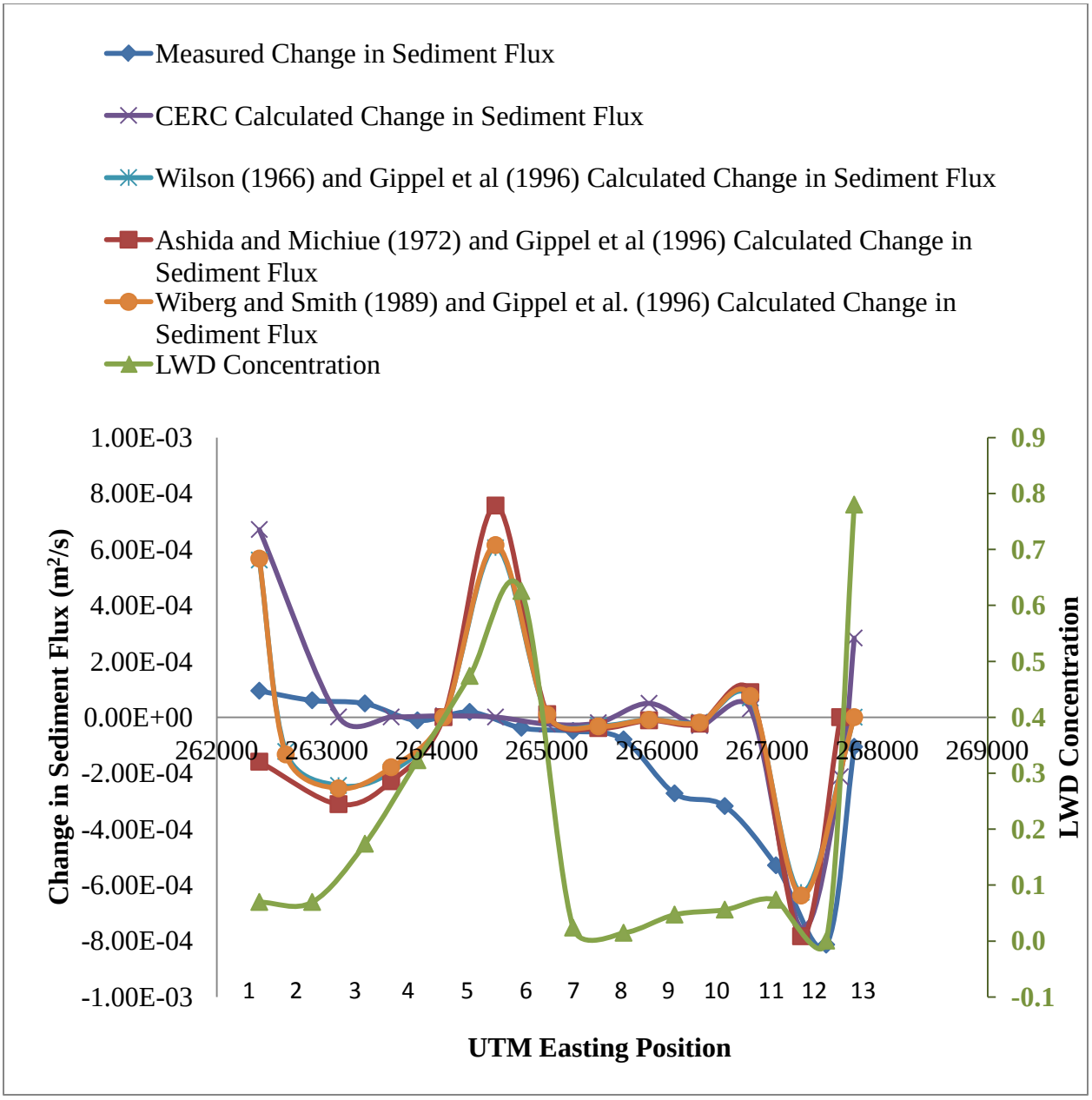

Figure 23: Both energetic (CERC) and mechanistic modeled change in sediment transport rates are plotted against the measured change in sediment transport rates (dark blue with squares) and large woody debris concentrations (plotted in green against the secondary axis). LWD generally correlates with a damped change in sediment flux, areas with low LWD have observed and predicted erosion. There appears to be a similar trend between the CERC predicted change in sediment transport rate and the mechanistic model's change in sediment transport rate based on changes in stress associated with LWD concentration. This correlation implies congruence between geometry of the delta and concentration of LWD, a relationship that should be researched further.

Figure 24: A truck on the eastern half of the modern Brazos delta, which is the side accessible by humans. In general, this side is stripped of LWD as collectors use the wood for burning. The inaccessible side of the delta (the western half) is the focus of our current study.

Figure 25: Tetrapods and similar concrete structures are emplaced along the shoreface and used to attenuate wave energy (Photos of Tokyo's tetrapods by Mike Beddal, 2009).